Report 25.5-01-06 Steel Fiber Reinforced Concrete Cylinders Under Uniaxial Compressive Loading – Preliminary Tests

Maart 2001

Dipl.-Ing. P. Schumacher / Dr.ir. drs. C. R. Braam / Prof. dr.ir. J. C. Walraven

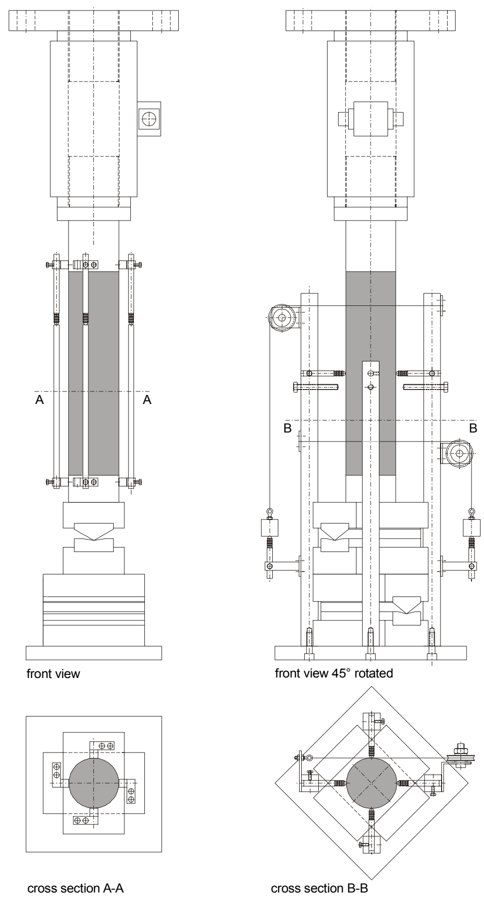

Delft University of Technology
Faculty of Civil Engineering and Geosciences
Section Concrete Structures

Report No. 25.5-01-06
Public
Project No. 3.00.01
March 2001

Steel Fiber Reinforced Concrete
Cylinders Under Uniaxial Compressive Loading – Preliminary Tests

External report
Financer: Delft Cluster (Delft Cluster project number 01.06.03)

External report

Authors:
P. Schumacher
C. R. Braam
J. C. Walraven

Delft University of Technology
Faculty of Civil Engineering and Geosciences
Section Concrete Structures

Report No. 25.5-01-06
Public
Project No. 3.00.01
March 2001

Steel Fiber Reinforced Concrete
Cylinders Under Uniaxial Compressive Loading – Preliminary Tests

Authors:
P. Schumacher
C. R. Braam
J. C. Walraven

TU Delft
Faculty of Civil Engineering and Geosciences
Section Concrete Structures
Stevin laboratory
P.O. Box 5048
2600 GA Delft
Telephone:015 2783990/4578
Fax: 015 2785895/7438

TABLE OF CONTENTS **Pag.**

1 Introduction

1.1 Scope of the research

This project is part of a research program on underground structures. Research is being done on the application of new materials in bored tunnels, especially steel fiber reinforced concrete (SFRC). Because existing material models for SFRC do not describe with sufficient accuracy all aspects relevant for the design of SFRC structures, more research has to be done. This research project deals with structural aspects on the redistribution of forces and the formation of plastic hinges. Therefore, the compressive softening behavior of SFRC was investigated. The two main goals of this research are:

1. Research on the behavior of steel fiber reinforced concrete prisms subjected to centric or eccentric compressive loading. The goal is to describe the softening behavior of the prisms and to make the Compression Damage Zone model applicable for fiber reinforced concrete.
2. Research on SFRC tunnel segments subjected to normal and bending forces as input for a model that describes the rotation behavior in the Ultimate Limit State.

With the knowledge thus acquired it will be possible to optimize the design of SFRC tunnel segments and the tunnel lining manufactured on the building site.

In order to do the prism experiments in such a way that the actual behavior is simulated with sufficient accuracy, the question arose whether the test specimens should be cast in moulds or sawn from bigger blocks. Both ways of manufacturing were used by other researchers in the past but no comparative study could be found on how large the differences in the results are.

It was therefore decided to do experiments on the wall effects in SFRC cylinders under uniaxial compressive loading.

1.2 Scope of this report

The way in which a test specimen is produced usually has a significant effect on the test results. In order to make realistic and safe design rules it is therefore important to know how the material behaves as test specimens and how this behavior should be translated to the actual behavior of a structure.

There are several ways to produce test specimens for the investigation of the softening behavior of concrete under compression. The easiest way is to cast them in moulds that already have the size needed for the test specimen. Another possibility, which is used by many researchers, is to saw or drill them from blocks of concrete to avoid wall effects.

The experiments described in this report were carried out in order to find out which influence the way of producing the test specimens has on the results of compressive tests performed on SFRC cylinders.

It was intended as a study preparing for the main research on centrically and eccentrically loaded prisms to be carried out later.

1.3 Outline of the report

Chapter 2 gives an overview of the recommendations for manufacturing test specimens, which are available at the moment, and of the ways in which other researchers manufactured the test specimens in their research. Chapter 3 and the appendices give information about the experiments that were carried out in order to determine the softening behavior of concrete cylinders subjected to uniaxial compression. The results of these experiments are given in chapter 4 and discussed in chapter 5. Chapter 6 presents the conclusions of this report. A summary of the report can be found in chapter 7.

2 Background

2.1 Preparation of the test specimens for uniaxial compression tests

The way of manufacturing the test specimens affects the test results [Van Mier, 1997, p. 205]. According to the RILEM[1] recommendation for tests designed to determine the strain softening behavior of plain concrete under uniaxial compression [RILEM, 2000, p. 348-349], there are two possibilities to manufacture the test specimens:

(1) casting them directly in the size required for the tests,
(2) sawing them from larger blocks.

In the RILEM recommendation, the second alternative is preferred.

When prismatic specimens are cast, they should be cast horizontally in order to get flat and parallel loading surfaces. A maximum deviation of 0.05 mm is accepted with regard to flatness of the loading surfaces. Cylinders can only be cast vertically and the casting surface must be ground flat so that it is parallel to the lower loading surface [RILEM, 2000, p. 348-349]. The most accurate surface smoothness can be obtained when steel moulds are used [Van Mier, 1997, p. 204].

If the prismatic specimens are sawn or if cylindrical specimens are cored from a larger block, the dimensions of the block should be at least two maximum aggregate sizes larger than the specimen dimensions needed. The best quality control on flatness and parallelness of the surfaces is possible when the specimens are sawn from larger blocks and then prepared in the following way: The specimens should be sawn 0.1-0.2 mm larger on all sides than required. Then the specimens should be ground to the size needed. This is supposed to lead to a good result so that capping between specimen and loading platen is not needed.

Van Vliet and Van Mier [1995, p. 8] used a procedure similar to the sawing of the test specimens described in the RILEM recommendation. They cast prisms made of plain concrete with a length of 600 mm and a cross-section of 150 mm * 150 mm. To produce the test specimens, they first sawed the outer 20 mm from each side and 100 mm from top and bottom ends to avoid wall effects. The top and bottom ends of the specimens were ground to obtain a good contact between specimen and loading platen. The sides of the specimens were also ground in order to facilitate adjustment of the transducers on the specimen.

---

[1] RILEM is an organization that aims at bringing together specialists from research and industry to promote progress in the design, testing, manufacture and use of building materials. For further information see web site http://www.ens-cachan.fr/~rilem/profile.htm .

Van Mier [1997, p. 204] describes in detail how the specimen surface should be treated. A specimen should be sawn from a larger block, removing a layer the thickness of which is at least once the maximum aggregate size. If the surface smoothness is not sufficient after sawing, it is necessary to grind the surfaces with a diamond grinding wheel. To make the surface even smoother, it can be impregnated with a low-viscosity epoxy and then be polished again. The result (or reward) of this procedure is little scatter in test results. Van Mier emphasizes that in the case of compression tests, the specimens should have a high surface smoothness to avoid contact difficulties with the loading platens. Some of these difficulties are shown in fig. 1. If the equipment available cannot produce such an accurate surface, a capping of rapid hardening cement or filled epoxy can be applied.

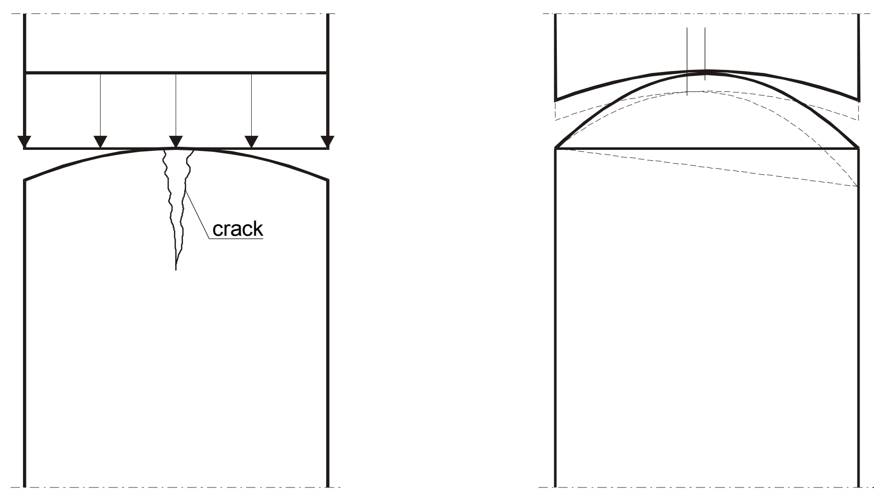

Fig. 2.1: Difficulties in loading a test specimen when the surfaces are not exactly flat and parallel

A BRITE/EURAM project about fiber reinforced concrete [BRITE/EURAM subtask 1.1, 1992, p. 15] reports that the fiber orientation depends on the method of casting and on the dimensions of the specimens. This can be explained by the fact that near a surface, the fibers are predominantly oriented parallel to the surface. The tensile forces in the center of the specimen resulting from outside compressive forces are carried by the more or less randomly oriented fibers in the center of the specimen. When a specimen is loaded eccentrically outside the core (i.e. the area where compressive forces only cause compressive and no tensile strains), tensile forces in the sides of the specimen are carried by the fibers that are oriented parallel to the sides of the specimens. In this case, it would therefore be a beneficial orientation. This is illustrated in fig. 2.2.

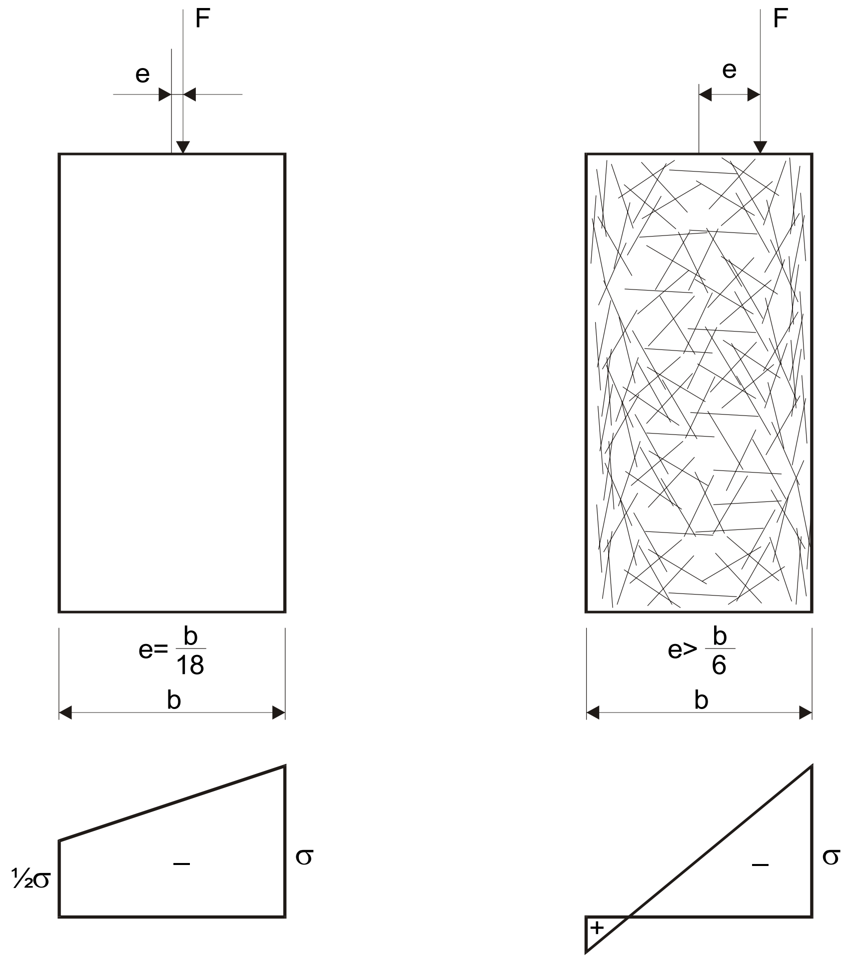

Fig. 2.2: Test specimen with load and corresponding strain distribution
left: load inside the core
right: load outside the core

In the scope of this BRITE/EURAM project, several researchers had their test specimens manufactured in the following way [Lin, 1999, p. 37; Lohrmann, 1998, p. 73; BRITE/EURAM subtask 1.1, 1992, p. 15]: Concrete blocks 1060 mm * 1060 mm * 300 mm were cast. Cylinders with a diameter of 100 mm were drilled from these blocks and the ends of the cylinders were grinded to a length of 250 mm.

Glavind cast cylinders for compression tests in plastic moulds with a diameter of 100 mm and a length of 200 mm. The moulds were removed one day after casting. The ends of the cylinders were grinded plane before testing [Glavind, 1992, p. 53].

2.2 Anisotropy effects due to the direction of casting

In the BRITE/EURAM research [see Lin, 1999; Lohrmann, 1998], the cylinders were drilled vertically and horizontally from the blocks. This was done in order to investigate the influence of the different fiber orientation on the test results.

3 Experimental set-up

3.1 The test specimens

3.1.1 Size of the test specimens

The original plan was to make test specimens in a prism shaped form with a size of 150 mm * 150 mm * 600 mm.

Reasons
There were several reasons to choose this specimen size. Firstly, the research is based on the research Markeset carried out [Markeset, 1993]. She used prisms with a size of 125 mm * 175 mm * 600 mm. The size of our test specimens was supposed to be in the same range. A practical reason was that the prisms with a size of 150 mm * 150 mm * 600 mm were cost-effectively to produce because the moulds were available since this is the standard testing size of bending beams [RILEM, 2000, p. 3. CUR Aanbeveling 35]. The size chosen was also in accordance with the requirements for minimum and maximum dimensions for the test specimens.

Requirements for minimum size
Different authors suggested different requirements concerning the minimum test specimen size. Kooiman [1998a, p. 4] suggested that the size of the test specimen should be at least five times the largest component (usually aggregate, here fiber). In the case of 30 mm long fibers this suggests a test specimen dimension of at least 150 mm in every direction.
The factor - five times the largest aggregate - was also suggested in the RILEM recommendation for testing the strain softening of concrete [RILEM, 2000, p. 348]. They consider this a representative volume of concrete, i.e. the specimen can be assumed to consist of a homogenous material.

According to ACI Committee 544 [ACI, 1988, p. 585], the size of the test specimens should be at least three times the larger of the fiber length and the maximum aggregate size.

Past research at TU Delft showed that larger test specimens had less scatter than smaller ones did. This effect was explained by the fact that at bigger dimensions of the test specimens the wall effects are smaller and the way of compacting has less influence [Kooiman, 1997, p. 15].

Requirements for the minimum length of the specimens
In order to avoid an inappropriate boundary effect from the loading platens in the failure zone, the specimen has to have a certain length in relation to its cross-section. According to the RILEM recommendation [RILEM, 2000, p. 348], the specimen length should be twice the diameter. Other researchers [Lin, 1999, p. 38; Lohrmann, 1998, p. 225] chose 2.5 times the cross-sectional dimension for the length.

Requirements for the maximum size
In theory there is no limit to the specimen size. For practical reasons, the size chosen to be 150 mm * 150 mm * 600 mm is rather large. Specimens larger than 150*150*600 mm are difficult to handle[2].

Specimens chosen
It was intended to cast the specimens in moulds as well as to saw them from a bigger block in order to determine whether the wall effects have an influence that needs to be considered.
Because sawing test specimens of this size was not possible with the concrete saw available in our laboratory, we decided to first do experiments with smaller test specimens on whether the wall effect has to be taken into account and then go on to the bigger prisms (which according to the outcome of the pre-tests would then be directly cast in the moulds or sawn from a bigger block).

In order to stick to the same length/diameter ratio we chose the test specimens to be cylinders with a diameter of 75 mm and a length of 300 mm.

According to the RILEM recommendation, the most convenient test specimen shape to measure the strain-softening behavior of concrete under uniaxial compression is a prism or a cylinder. The size of the specimen should be so large that a representative volume of the concrete is taken. The characteristic dimension of the cross-section should be at least five times the size of the maximum aggregate. The length of the specimen should be twice the characteristic cross-sectional dimension [RILEM, 2000, p. 348].

Cylinder size
The size of the first test cylinders was chosen to be 74 mm in diameter and 300 mm in length. The moulds for the cylinders that were to be cast had an inside diameter of 74 mm and a height of 412 mm. After demoulding and cutting, the cylinders had a size of 74 mm in diameter and 300 mm in length. The cylinders that were drilled from a bigger block were cored with a drilling machine with a diameter of 74 mm. The vertically drilled cylinders were cut to a length of 300 mm. The horizontally drilled cylinders already had a length of 300 mm.

3.1.2 Number of test specimens and parameters that were varied

The number of test specimens per experiment was chosen to be four. At least three test specimens per experiment are usually required, e.g. in RILEM [2000, p. 351].
We chose to carry out every experiment with four test specimens in order to get a realistic average result even if an LVDT fell off one of the specimens. This helped to take the scatter into account.

According to the RILEM recommendation [RILEM, 2000], the specimens can either be cast directly of the size required in the tests, or as a (preferred) alternative, the specimens can be sawn from larger blocks. In order to find out about the influence of the casting direction and the surfaces of the test specimens, the specimens were manufactured in the following ways:

---

[2] 150*150*600 mm weighs about 30 kg and can thus still be lifted by a worker in the laboratory. Heavier specimens would require more equipment [Kooiman, 1998b, p. 4]. Larger specimens need to be lifted by a machine and different test set-ups have to be built, especially when high concrete strengths are tested.

vertically and horizontally drilled cylinders
vertically drilled and vertically cast cylinders.

Due to the fiber orientation in a specimen, it was decided to investigate the differences between horizontally and vertically drilled cylinders. The cylinders that were directly cast in the moulds could only be cast vertically. They were compared to the cylinders that were drilled vertically from a bigger block.

3.1.3 Production of the test specimens

3.1.3.1 Moulds

The moulds used for the block from which cylinders were drilled had a size of 300 mm * 300 mm in cross-section and 350 mm in height. The plastic moulds used for casting cylinders had an inside diameter of 74 mm and a height of 412 mm. The moulds for the test cubes had a size of 150 mm * 150 mm * 150 mm.
All the moulds except the plastic moulds, which were used for the vertically concreted cylinders, were made of steel. The steel and the plastic moulds were oiled with a brush before casting. They were greased before the concrete was put in.

The test specimens were given the names CC 1 to 4 for the cast specimens, CV 1 to 4 for the vertically sawn specimens, and CH 1 to 4 for the horizontally sawn specimens.

3.1.3.2 Concrete mixture

The concrete mix was designed to be a B 45 (i.e. characteristic 28-day cube compressive strength 45 N/mm^2; 150 mm cubes). 110 liters were prepared.

The mix for 1 m^3 was:

Cement CEM I 52.5 R (ENCI Maastricht)	87.5 kg
Cement CEM III/B 42.5 LH HS (ENCI IJmuiden)	262.5 kg
water cement ratio = 0.45	
water	155.4 kg
Addiment FM951	2.8 kg

fractions		
8-16 mm	25 % (by weight)	488.85 kg
4-8 mm	24 % (by weight)	467.55 kg
2-4 mm	8 % (by weight)	149.62 kg
1-2 mm	18 % (by weight)	336.64 kg
0.5-1 mm	21 % (by weight)	392.74 kg
0.25-0.5 mm	2 % (by weight)	37.40 kg
0.125-0.25 mm	2 % (by weight)	37.40 kg

Total aggregate: 1910.21 kg

Fibers:
40 kg per m^3
Dramix RL-45/30-BN
The fibers used were straight fibers with hooked ends. They were produced by Bekaert, Belgium and had the product name Dramix RL-45/30-BN with

R: regular, i.e. with hooked ends
L: loose i.e. not glued together
45: aspect ratio = l_f/d_f = fiber length/fiber diameter
30: fiber length l_f [mm]
B: blank, i.e. without any anti-corrosion covering such as zinc
N: normal strength steel with a low carbon content
minimum tensile strength of 1000 N/mm^2

3.1.3.3 Production / Mixing

3.1.3.3.1 Dosage

The maximum amount that could be mixed in the free fall mixing machine at one time is 300 liters. For every mixture, sand and gravel were taken from the silos in the aggregate grading groups mentioned in the mix design. They were filled in a container in which they immediately could be weighed. Water, the cements and the steel fibers were weighed separately and later added to the aggregates. The accuracy of the scale was about 50 g.

3.1.3.3.2 Mixing and properties of the fresh concrete

The aggregates were put into the free fall mixing machine. The mixing machine was started and was running with the aggregates in it for about 30 seconds when the steel fibers, the water, and the superplasticizer were added. This was mixed for about one minute. Then, the cements were added, and the concrete was mixed for another 180 seconds. While the mixing machine was still running, the concrete was dumped into a wheelbarrow. This took 15 seconds. The mixing machine had to run while putting things into or out of the mixer.

The temperature of the fresh concrete was 21.6°C. Room temperature and relative humidity were not measured. The room temperature was about 20°C (outside temperature was a high of 16°C and a R.H. of about 80% that day).

The mixture was rather dry (as can be seen in appendix A1).

After mixing the concrete, the following properties were measured: slump, flow spread, and air content. The tests are explained on the following pages.

Slump test

The slump was measured to be 35 mm by using an Abrams' cone according to the Dutch standard NEN 5956 [NEN 5956, 1988].

The interior side of the cone and the table on which it was to be put were wetted with water. The concrete was put into the cone in three layers of 100 mm each. Each layer was compacted by letting a rod fall on it ten times. After the top layer was compacted the cone was filled so that just a little amount of concrete was over the rim of the cone. With the steel rod, the superfluous concrete was disposed of in a rolling/sawing movement so that the concrete was just as high as the rim of the cone. The table around the cone was cleaned. After about 30 seconds, the cone was lifted upwards. The concrete produced sank 35 mm.

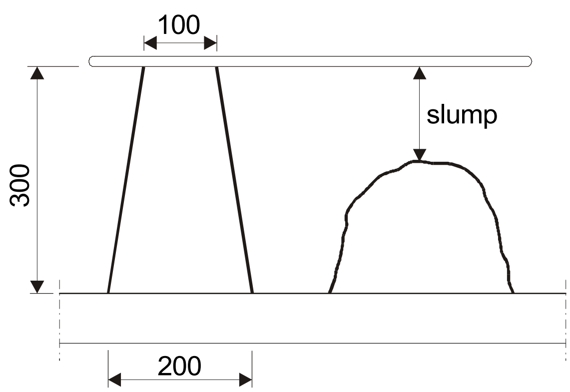

Fig. 3.1: Slump test [after: NEN 5956]. Dimensions in [mm].

Flow test

After the slump was measured, the table was lifted and let fall ten times in 30 seconds.
The diameters measured afterwards were 370 mm and 390 mm, respectively, thus flow was in average 380 mm [NEN 5957].

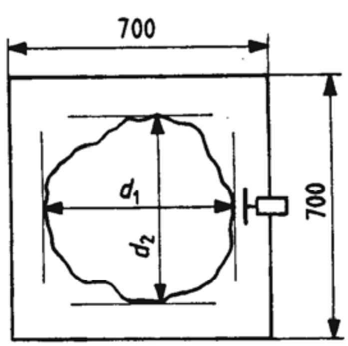

Fig. 3.2: Flow test [after: NEN 5957]. Dimensions in [mm].

Air content

The container was filled with concrete in one layer and compacted on a vibration table for 30 seconds. The surface of the concrete was made even with the rim of the container and the top was put on it. The air content meter was filled with water until all the air that was still in the closed container was out.

The air content was measured to be 2.7% according to the Dutch standard NEN 5962.

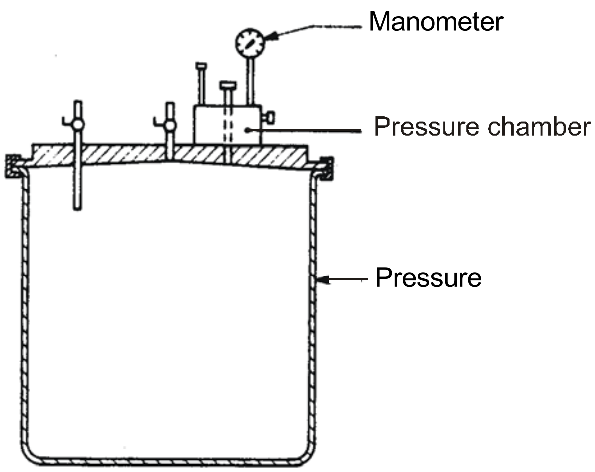

Fig. 3.3: Air content meter [after: NEN 5962].

3.1.3.3.3 Transportation

After the concrete had been dumped into a wheelbarrow, it was rolled next to the compaction table. From there, it was shoveled into the moulds with hand shovels.

3.1.3.3.4 Casting and compacting the test specimens

The cylinders that were cast vertically were concreted and compacted in one layer. This was a misunderstanding. It should have been done in three layers.

First, the container for the air content measurement was filled with concrete and compacted for 30 seconds. The air content was then measured to be 2.7 % (see above for details).
Then, the first steel mould for drilling the cylinders was filled with concrete and compacted for 30 seconds. When compacting the concrete, the concrete sank in the forms and more concrete was added while compacting. It was finished with a wet piece of metal and covered with a plastic sheet which was carefully placed on the concrete, wiping it with the hand from one side to the other (like when putting up wall paper) to avoid air entrapments.

Then, the mixing machine was run for another 15 seconds in order to be able to completely unload it. After this mixing, the second steel mould for drilling the cylinders was filled with concrete and compacted for 30 seconds.

Then, the four plastic moulds for the cylinders were filled with concrete in one layer and compacted for 30 seconds. When it was obvious that too much air was still in the specimens, they were compacted for another 30 seconds. While being compacted, the cylinder moulds were fixed to the vibration table by the workers in the lab by hand.
When compacting the specimens in steel moulds, the moulds were fixed to the vibration table with the help of pieces of wood.

At the end, 6 steel moulds for cubes with a length of 150 mm were filled with concrete, fixed to the vibration table and then compacted for 30 seconds.

The specimens for the cylinders were put on a pallet and then put in place where they could stay until demoulding two days later. The test cubes were put on a table until demoulding two days later. Putting plastic sheets or wet cloths is recommended in the RILEM recommendation [RILEM, 2000, p. 349].

It should be kept in mind that the external vibration used in these experiments can orient the fibers perpendicular to the direction of vibration [Kooiman, 2000, p. 11]. External vibration is, however, used because internal vibration leads to regions with fewer fibers.

3.1.3.3.5 Curing

The test specimens were covered with plastic to avoid moisture losses and left in the lab for two days until they were demoulded. The temperature in the lab was approximately 20°C.

3.1.3.3.6 Demoulding

The test cubes and the blocks for drilling the cylinders were demoulded two days after concreting. Then, they were placed in a fog room at 99% RH and 20°C. This was done according to the RILEM recommendation [RILEM, 2000, p. 349]. The cylinders that were concreted in the plastic moulds were left in the moulds and the moulds were placed in the fog room.

Right after demoulding, the moulds were cleaned and olied for the next time.

3.1.3.3.7 Storage

According to the RILEM recommendation [RILEM, 2000, p. 349], the specimens were stored in a fog room (99% RH at 20°C).

3.1.3.3.8 Further treatment (sawing, grinding)

The cylinders were drilled from the larger blocks 19 days after concreting. In the literature it was recommended to wait at least 7 days [Lohrmann, 1998, p. 73] or 14 to 21 days [RILEM, 2000, p. 349]. According to the RILEM recommendation [RILEM, 2000, p. 349], grinding of the loading surfaces is necessary to ensure flatness of the surfaces and good contact between specimen and loading platen. Sawing the specimen 0.1-0.2 mm larger than required on all sides and removal of the excess material by grinding is said to lead to good results. The casting surface should be marked. After sawing and grinding the specimens are to be returned to the fog room.

In the very first experiment, the ends of the test specimen were sawn only, without any additional grinding afterwards. Because problems occurred during this experiment we decided that the specimens need further treatment in the form of capping.

The specimens were sawn from the blocks according to the plan in appendix 2. The test specimens were marked with an identification code in order to be able to recognize their position afterwards. The direction of concreting and sawing were also marked on each test specimen. According to the RILEM recommendation, all dimensions of the specimen should be measured before the beginning of the test. The axial dimension should be measured in four places and the average from the four measurements should be given. The diameter should be measured on three positions [RILEM, 2000, p. 349]. The diameter of the specimens used here was 74 mm.

On the same day on which the cylinders were drilled from the larger blocks, the cylinders that had been cast in the plastic moulds were demoulded. All of the test specimens were returned to the fog room until testing.

3.2 Testing machine and testing

There are several criteria to choose a testing machine. They are given in [Kooiman, 2000, p. 24] and include the complexity of the test set-up, the preparation the specimens, the execution of the test, the reproducibility of the tests, the reliability of the test results, the costs of labor, the applicability in practice, and the acceptance of the test method by researchers. The testing machine should also have a high stiffness compared to the test specimens [Grimm, 1997, p. 28].

3.2.1 The testing machine

The testing machine and the very first test specimen can be seen in fig. 3.4.

Fig. 3.4: Testing machine and test specimen

The total loading capacity of the machine was 2000 kN. The capacity of the hydraulic jack was 2000 kN. The maximum load expected on the prisms was about 1.25 MN (B45 with a mean strength of 55 N/mm^2 * 150 mm * 150 mm = 1.24 MN).

The test specimens were put on the testing machine. A piece of wood (3 mm thick) was placed on top and bottom of the test specimen. On top of this, there was a steel loading platen (50 mm thick). The test specimen was evenly supported on the bottom. The loading platens were prepared according to the RILEM recommendation [RILEM, 2000] with teflon and grease according to fig. 3.5 with the difference that we used grease-teflon-grease instead of teflon-grease-teflon.

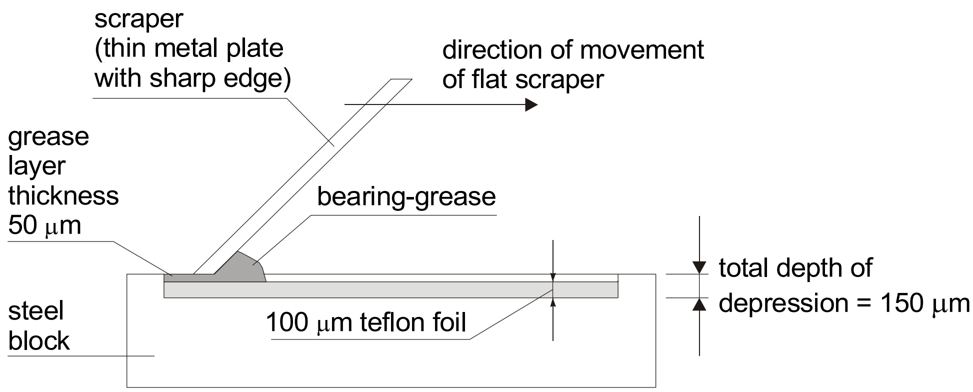

Fig 3.5: Preparation of the specimens [after: RILEM, 2000]

3.2.2 Number and position of measuring devices

All LVDTs measured the deformation at a certain load.

Four LVDTs (LVDT01 to LVDT04) were placed on the sides of the cylinder to measure the longitudinal deformation. They measured over a measuring length of 10 mm with an accuracy of 5/2048 = 0.002441.

In the middle of the specimen, four LVDTs (LVDT05 to LVDT 08) were placed on a stiff frame to measure the circumferential deformation. 100 mm above and below them, steel wires were placed around the specimen to measure the circumferential deformation as well (LVDT09 and LVDT10).

Because the LVDTs might fall off during experiments due to spalling at the surface of the specimen, we chose to measure the total longitudinal deformation rather than just measure it in the middle of the specimen.

The compressive force was measured by an electronic pressure applier with a capacity of 400 kN and a measuring accuracy of 400/2048 = 0.195313.

The axial deformation used in the feed-back signal was measured between the loading platens. The signal from LVDTs 01 to 04 was averaged.

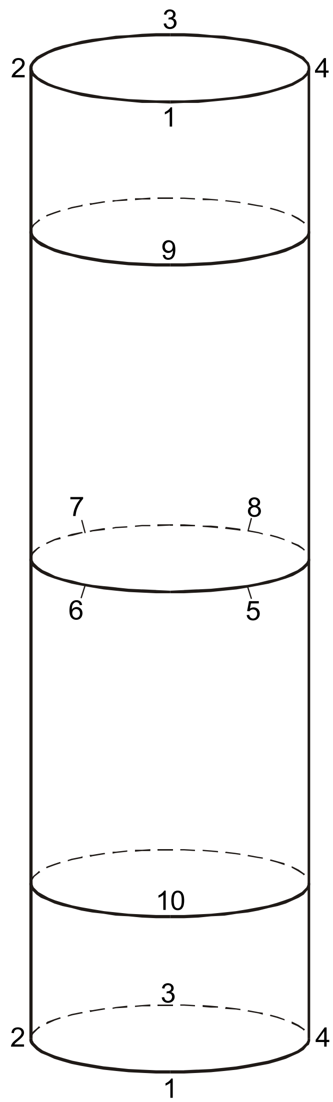

Fig. 3.6: Test specimen and numbering of the LVDTs

3.2.3 Control and speed of loading

The concrete cylinders were tested deformation-controlled as required in [RILEM, 2000, p. 350]. The speed was 1 μm/s, which was recommended in [RILEM, 2000, p. 350]. According to [BRITE/EURAM subtask 1.2, 1992, p. ii], the speed of deformation in static tests should be between 10^{-5} s^{-1} and 10^{-6} s^{-1}.

The LVDTs controlling the deformation were the vertical ones (see appendix A4). According to [RILEM, 2000, p. 350], the axial deformations can be used as control signal for conventional normal gravel concretes with a compressive strength up to about 70 N/mm^2. For higher strengths, three alternatives exist: control over the circumferential or lateral deformation, control over a combination of axial load and axial deformation, or control over a combination of axial and lateral deformations.

No single method is preferred in the recommendation. In our case, normal strength concrete was tested and therefore it was decided to use the longitudinal deformation as control parameter. A closed-loop test set-up was used in the experiments.

3.2.4 Boundary conditions

The RILEM recommendation states that the peak stress as well as the post-peak softening curve are highly dependent on specimen geometry and boundary conditions during the experiment. The specimen behavior becomes more ductile when the boundary restraint is increased [RILEM, 2000, p. 347]. It was therefore chosen to manufacture the loading zones as recommended in [RILEM, 2000, p. 351] and shown in fig. 3.7.

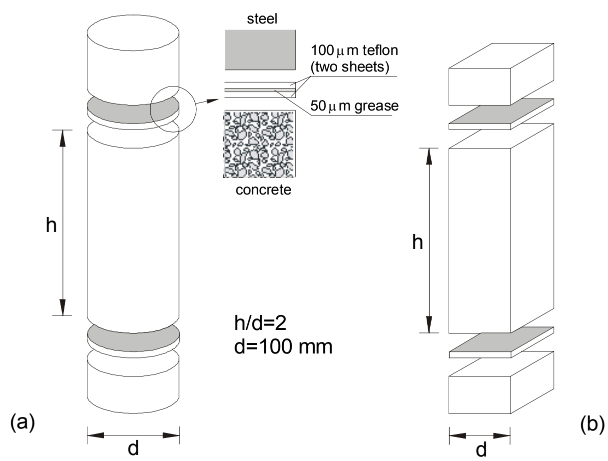

Fig. 3.7: Standard test for measuring softening of concrete in uniaxial compression [after: Van Mier, 1997, p. 251]

One deviation from the RILEM recommendation was made: in all tests (except test specimen CC 2), we used two layers of grease with one layer of teflon in between instead of the recommended two layers of teflon with one layer of grease in between.

3.2.5 Age of testing

Due to problems with the initial test set-up, the tests were not performed at the planned age of 28 days but at an age of about 110 days. The reference cubes were tested right after all cylinders had been tested.

4 Results

This chapter presents a summary of the test results.
To make it easier for the reader to compare them, different figures presenting the same phenomenon are given in the same layout even if a different scaling of the axes would make more sense for a particular figure.

The curves given in chapter 4.1 are the average curves of the four *longitudinal LVDT's* of each test. This was also the control signal. The curves of LVDT 01 to LVDT 04 are given in appendix A5.

In most cases, the load *eccentricity* at peak load was within ± 1 mm of the center of the specimen. An example is given in chapter 4.2 and the curves are given in appendix A6.

In most cases, the *lateral deformation* up to peak load also stayed within the range of ± 1mm. After the peak load, the deformations increased. The shape of the curves is explained in chapter 4.3 giving examples. The curves are given in appendix A7 (for LVDTs 05 to 08) and appendix A8 (for LVDTs 09 and 10).

The pictures of the test specimens are given in appendix A9. The names of the test specimens are explained in appendix A3.

4.1 Load – longitudinal deformation diagrams

The curves given in this chapter are the average curves of the four longitudinal LVDTs of each test. This was also the control signal. The curves of LVDT 01 to LVDT 04 are given in appendix A5.

1 mm deformation over a measuring length of 300 mm is equal to a strain of 3.33 $^{o}/_{oo}$.

A force of 170 kN corresponds to a stress of $0.17\ \text{MN} / (0.25 * \pi * 0.074^2\ \text{m}^2) = 31\ \text{MN/m}^2$.

In all cases concrete spalled off.

4.1.1 Vertically cast cylinders

Fig. 4.1 shows the results of the compression tests on vertically cast cylinders:

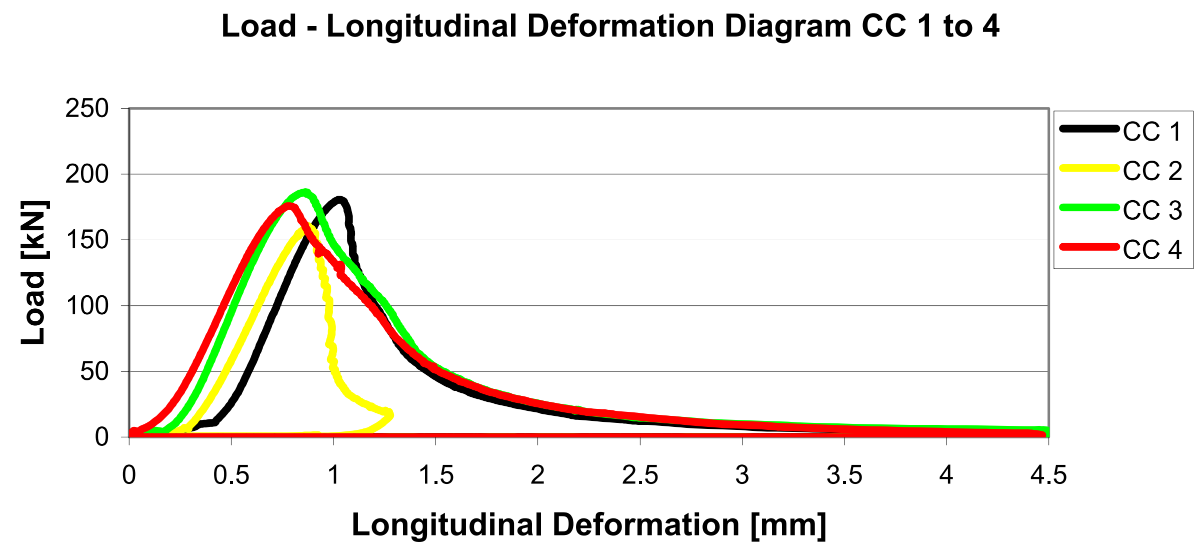

Fig. 4.1: Load – Mean Longitudinal Deformation Diagram of the compression tests on vertically cast cylinders

The tests CC1, CC3, and CC4 ran according to the method described in chapter 3.

CC 2 is an exception in a way since it was the only test specimen which was tested with two layers of teflon and a layer of grease in between (according to the RILEM recommendation mentioned in chapter 3.2.4). All other tests were done with two layers of grease and a layer of teflon in between.

4.1.2 Vertically drilled cylinders

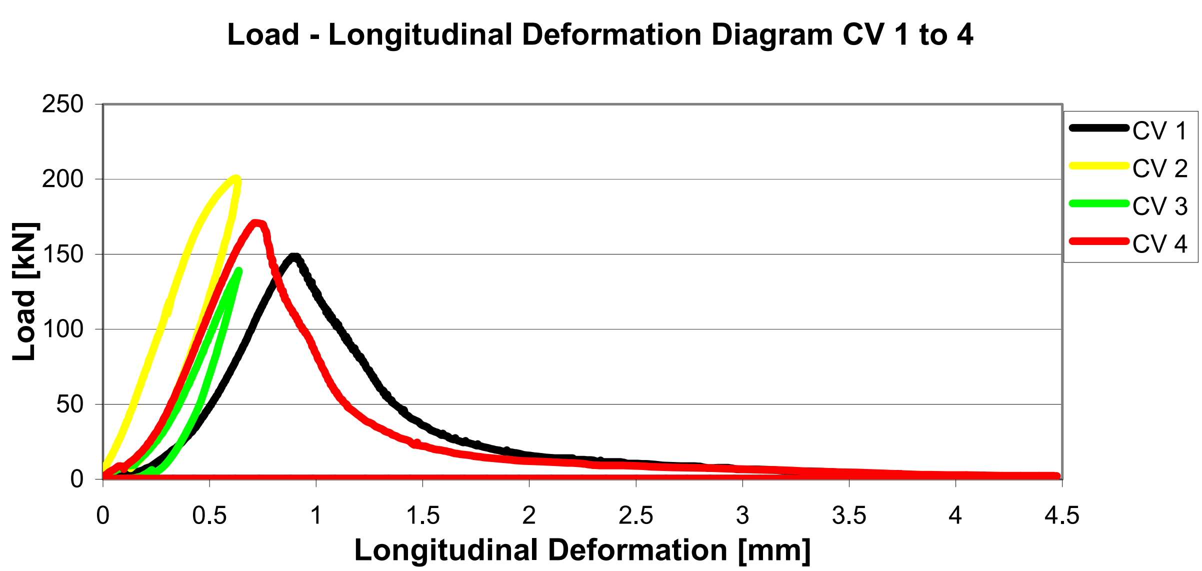

Fig. 4.2: Load – Longitudinal Deformation Diagram of the compression tests on vertically drilled cylinders

The tests CV 1 and CV 3 ran according to the method described in chapter 3.
The test specimens CV 2 and CV 4 failed suddenly.

4.1.3 Horizontally drilled cylinders

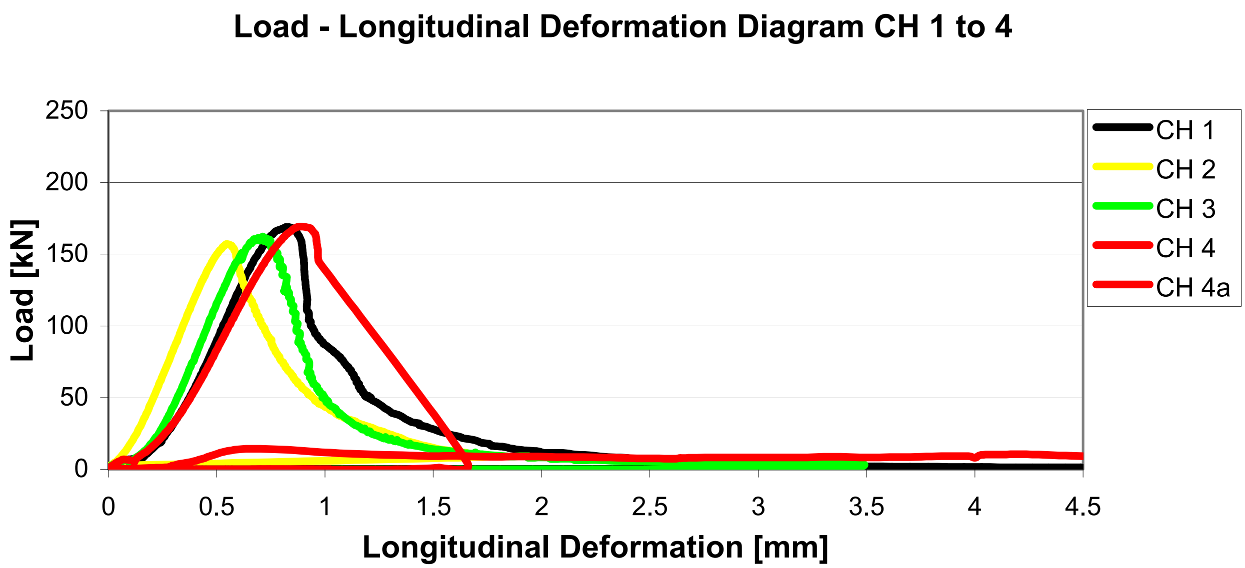

Fig. 4.3: Load – Longitudinal Deformation Diagram of the compression tests on horizontally drilled cylinders

The tests CH 1, CH 2, and CH 3 ran according to the method described in chapter 3.
CH 4 failed explosively at about 140 kN on the descending branch. The test was stopped and started again (CH 4a).

4.2 Eccentricity of the loading

In most cases, the load eccentricity at peak load stayed within ± 1 mm of the center of the specimen. The curves are given in appendix A6. One example is given here:

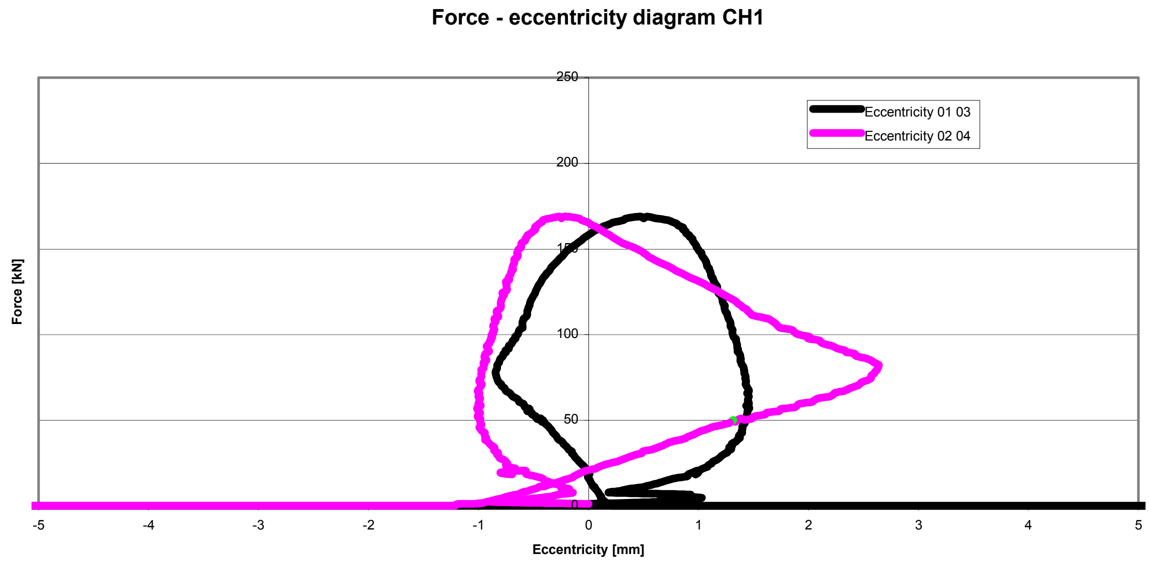

Fig. 4.4: Load – Eccentricity Diagram of the compression test on the horizontally drilled cylinder CH 1

The eccentricity was calculated from LVDT 01 and 03 (e_1) in one direction and from LVDT 02 and 04 (e_2) perpendicular to it. Assuming that the longitudinal deformation varies linearly in between two LVDTs, the total eccentricity was calculated from the single eccentricities:

$$e_{total} = \sqrt{e_1^2 + e_2^2}$$

An example of this is given in fig. 4.5.

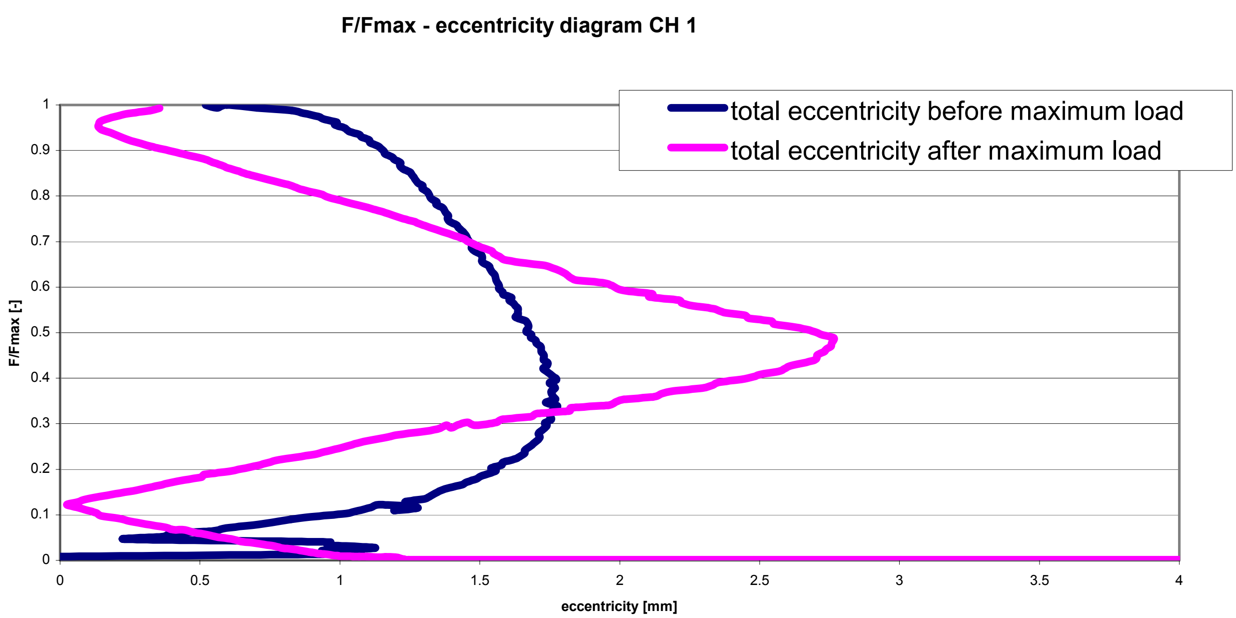

Fig. 4.5: Load / maximum load – total eccentricity diagram of the compression test on the horizontally drilled cylinder CH 1

In fig. 4.5, it can be seen that the test specimen first tries to find its way and then is loaded nearly centrically.

4.3 Lateral deformation

In most cases, the lateral deformation up to peak load also stayed within the range of ± 1mm. After the peak load, the deformations increased. The shape of the curves is explained in section 4.3.1 giving examples. The curves are given in appendix A7 (for LVDTs 05 to 08) and appendix A8 (for LVDTs 09 and 10).

4.3.1 Lateral deformation measured in the middle of the specimens (LVDT 05 to 08)

Fig. 4.6 gives an example of the lateral deformations measured at a test specimen:

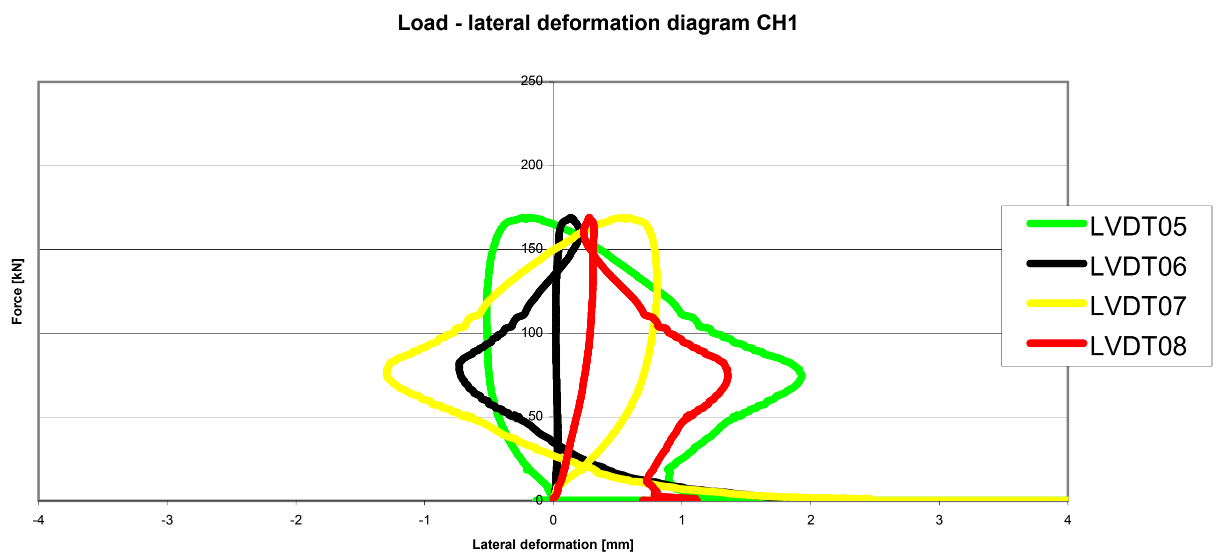

Fig. 4.6: Load – lateral deformation diagram of the compression test on the horizontally drilled cylinder CH 1

Before the peak load, the lateral deformation was observed to follow the following pattern:
When a certain LVDT was pushed on one side, the LVDT on the opposite side was released somewhat.
After the peak load, the deformations increased and after some time, all LVDTs were pushed.

4.3.2 Lateral deformation measured on top and bottom of the specimens (LVDT 09 and 10)

From LVDT's 9 and 10 measuring the length of the wire around the test specimen it can be seen that failure localizes in one place while the other LVDT does not show much movement.

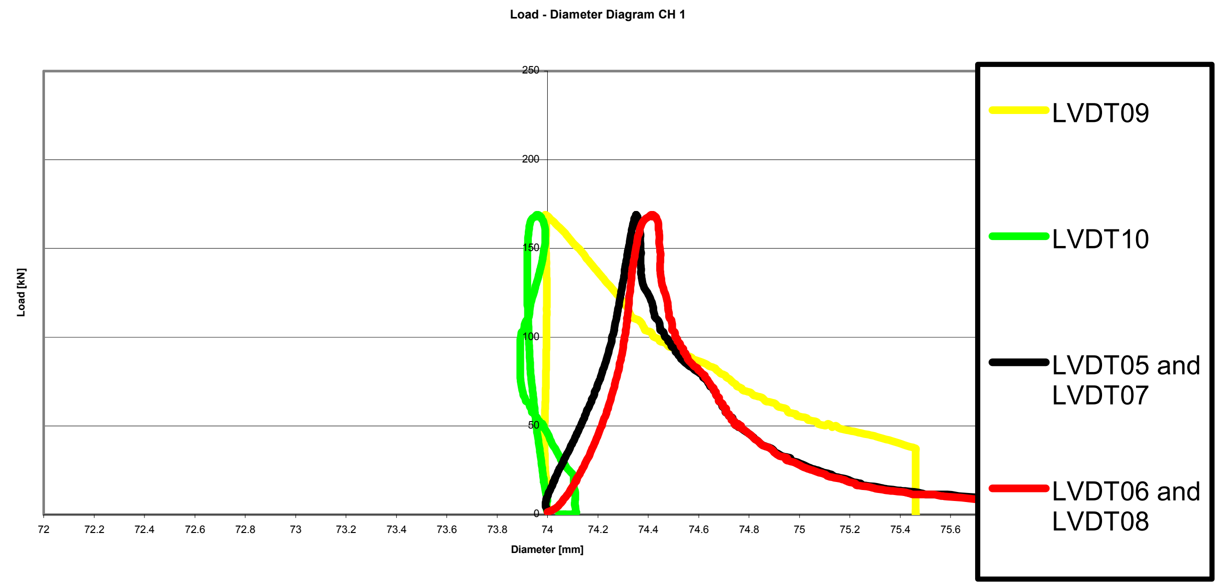

Fig. 4.7: Load – diameter diagram of the compression test on the horizontally drilled cylinder CH 1

The diameters given in fig. 4.7 were calculated from the results of the measurements of LVDTs 05 to 10.
The figure shows that for test specimen CH 1, failure occurred mainly on the side where LVDT 09 measured. On the bottom of the specimen, nearly no change in diameter was registered.

4.4 Test cubes

The six cubes were tested at an age of 118 days, which was right after the cylinder tests had been completed. Three cubes were tested for compressive strength and three for tensile splitting strength.

The mean compressive strength of the three cubes was 63.2 N/mm^2 with a standard deviation of 1.2 N/mm^2.

The mean tensile splitting strength was 3.7 N/mm^2 with a standard deviation of 0.3 N/mm^2.

5 Discussion

This chapter is divided into two parts. First, the data obtained in the tests were processed in order to interpret and compare them. This is explained in chapter 5.1. Then the processed data are discussed in chapter 5.2.

5.1 Processing the data

In this chapter, a procession of the test data is explained. This procession is the basis of comparing the test results in chapter 5.2 (discussion).

Processing the initial increase of deformations
The load – displacement curves were processed in order to separate the influence of the boundary condition from the specimen behavior. As the load increases, the axial deformations increase faster than expected in most tests. This behavior can be explained by the fact that the teflon layer with a thickness of 0.1 mm and the layers of grease have to be compressed before the loading platens are in contact with the test specimens. As soon as the contact between loading platen and test specimen is established, the longitudinal deformations increase with the force according to the expected concrete stiffness.
To do this, a straight line was drawn through the points of the curve at 30% and 40% of the maximum load (to represent the concrete stiffness). The load – deformation curve was then shifted to the left by the value of the x-axis where this line crosses it.
Another step that could be taken (but is not taken here) is to replace the initial part of the load – displacement curve by a straight line. This looks nicer but has no effect on the test interpretation. Furthermore, it may confuse the quick reader.

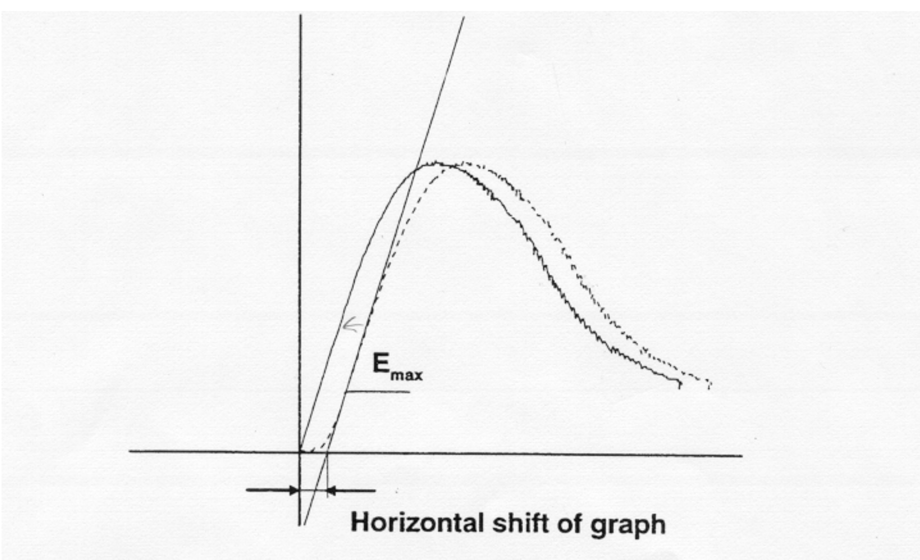

Fig. 5.1 Correction of the initial slope of the load-displacement curve (compare to van Vliet & van Mier, 1995, p. 10)

Other possible ways of processing the data
Another possible way of processing the data which is not made here is to substract the elastic deformation of the part of the steel loading platen that was within the measuring range (here 20 mm = 10 mm from above + 10 mm from beneath the specimen) from the total deformation. Additionally, the measurements are influenced by the deformation of the teflon layer and the grease layer.
All these deformations are not taken into account because they are very small compared to the deformations measured.
$\delta_{elastic}$ = F [N] * 20 [mm] / (E_{steel} * A) = 200000 N * 20 mm / (205000 N/mm^2 * 0.25 * π * 74^2 mm^2) = 0.004539 mm = 4.539 µm
For further information:
A comparison of the behavior of the loading conditions steel (high friction) and teflon-grease-teflon (low friction) can be found in van Vliet, van Mier, 1995, p. 10-11.

The results thus obtained are given in figs. 5.2 to 5.4.

Furthermore, to mutually compare the shapes of the curves of individual specimens, on the vertical axis the relative force is given (F/F_{max} with F_{max} is the maximum load carried by a specific specimen).

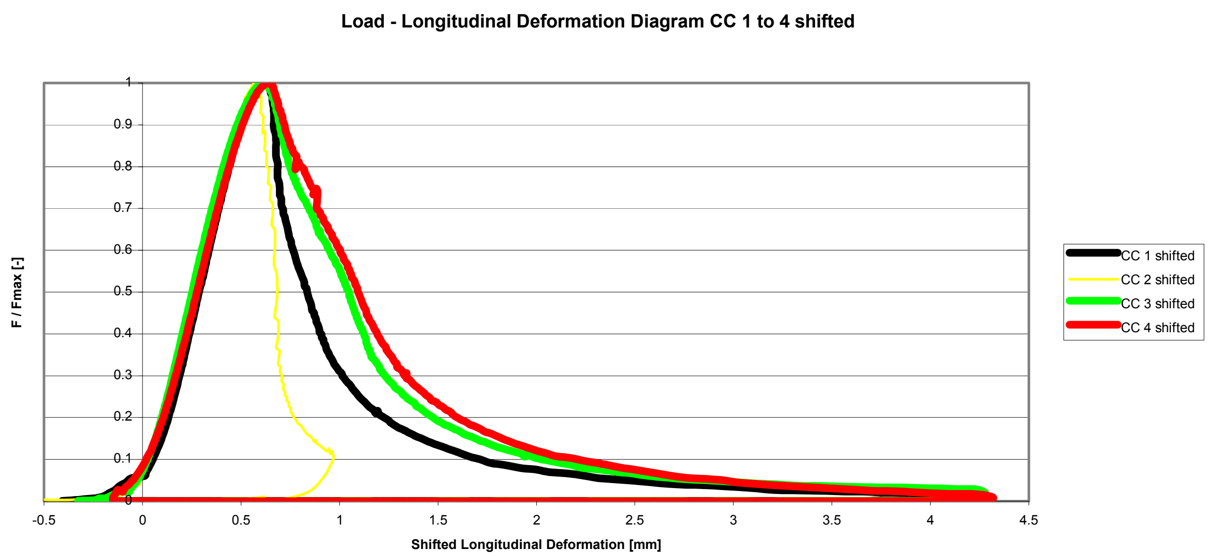

Fig. 5.2: Load – longitudinal deformation diagram CC1 to CC 4, shifted

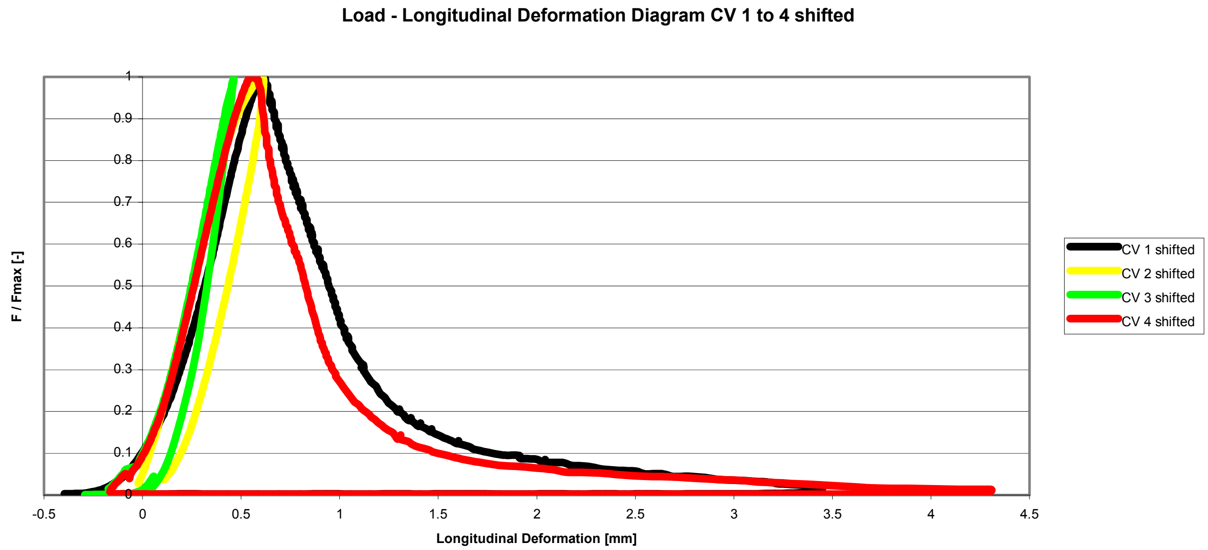

Fig. 5.3: Load – longitudinal deformation diagram CV1 to CV 4, shifted

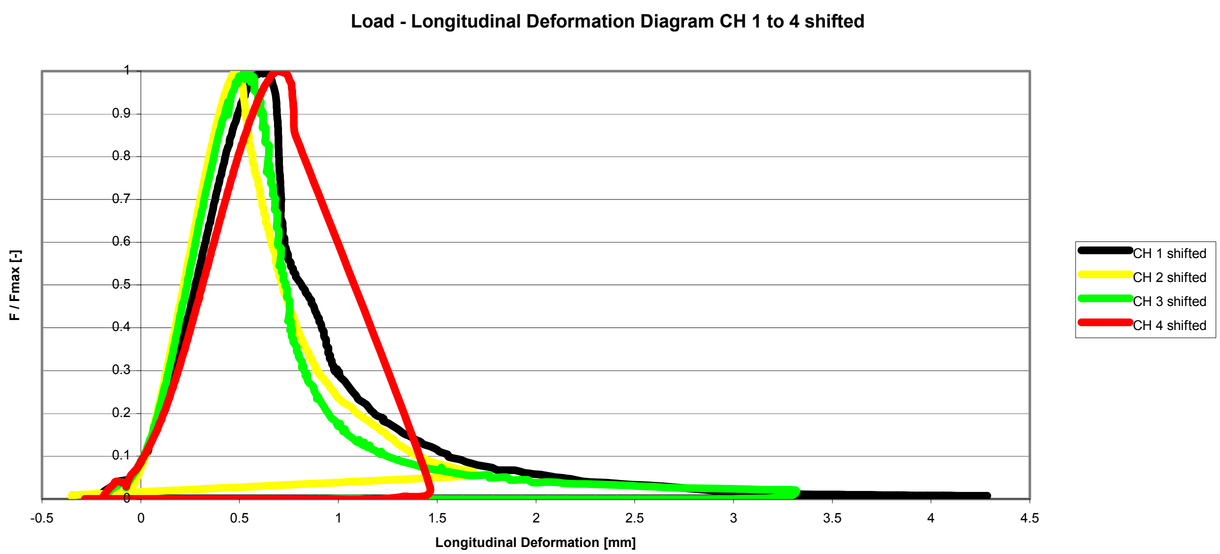

Fig. 5.4: Load – longitudinal deformation diagram CH 1 to CH 4, shifted

CH 4

Because the test specimen CH 4 suddenly failed at a load of about 140 kN on the descending branch and the test was then started again (named CH 4a in chapter 4) the descending branch of CH 4 does not represent the real concrete behavior.

In order to compare the different ways of manufacturing the test specimens with each other, we put trendlines through the shifted data for the load – longitudinal deformation measurements.
The trendlines are polynomials of the ninth order and the curves had to be split into three parts each in order to achieve polynomials that fit the original shape of the curves.

The tests in which the descending branch of the load – deformation curve could not be measured are left out of consideration.

The trendlines found with this procedure are given in fig. 5.5.

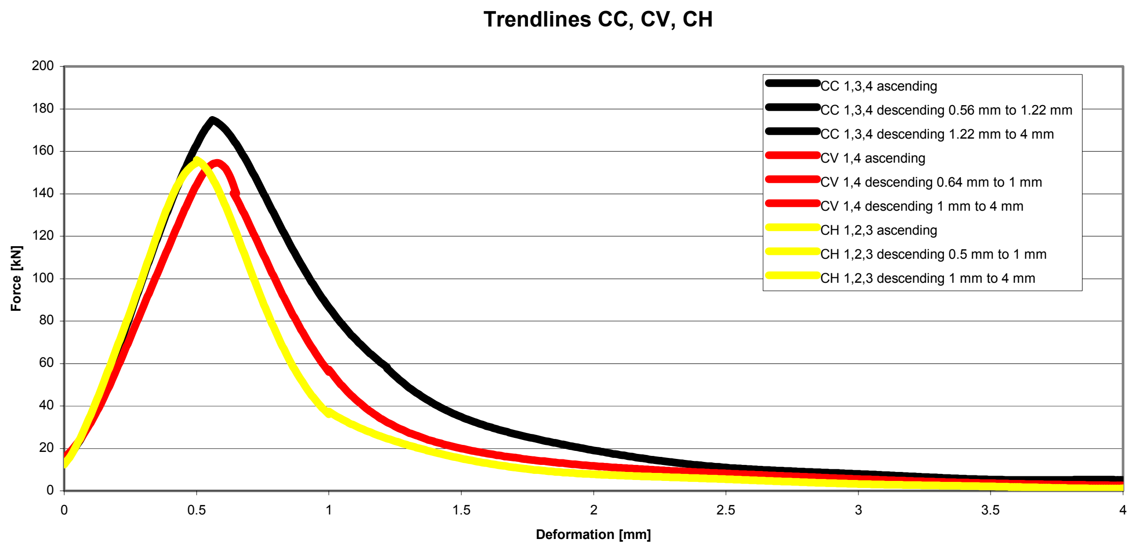

Fig. 5.5: Trendlines through the results from the load – longitudinal deformation measurements of different ways of manufacturing the test specimens

Then, the data in which the normalized force F / F_{max} and the longitudinal deformation are given were processed. Because the original test data varied in x- as well as in y-values, we used linear interpolation to get the x-values for given y-values. Then, these x-values were averaged for each production method. The thus acquired diagrams can be seen in fig. 5.6.

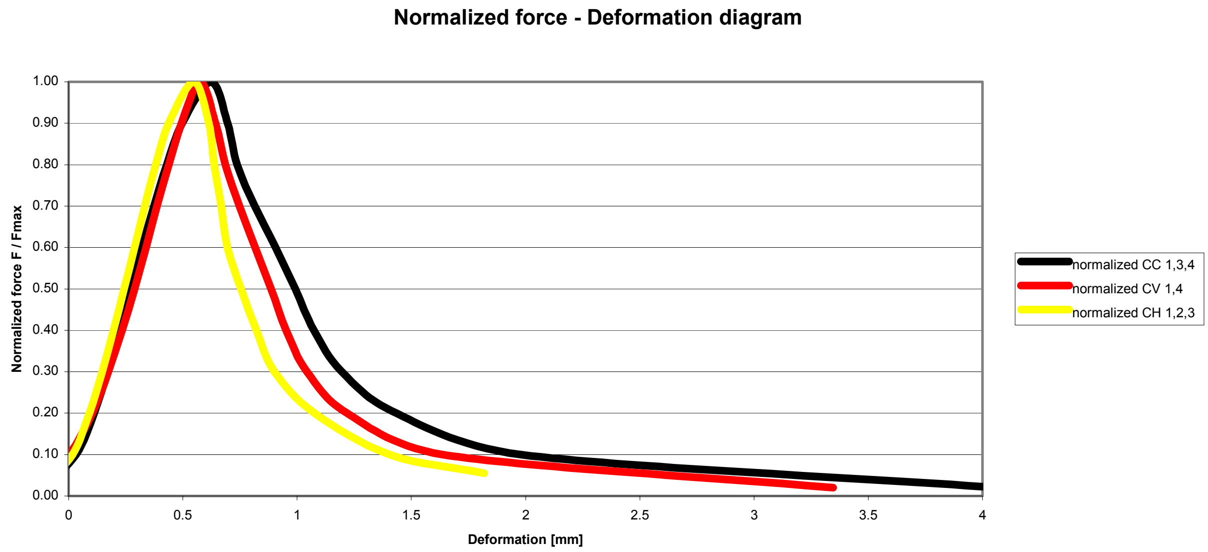

Fig. 5.6: Average lines from the test results for force – longitudinal deformation measurements: normalized force F / F_{max} – deformation diagram

In order to better compare the shape of the load – longitudinal deformation diagrams of the different production methods, we also normalized the deformation with regard to the deformation at peak load of each individual test.

The outcome of this modification can be seen in fig. 5.7.

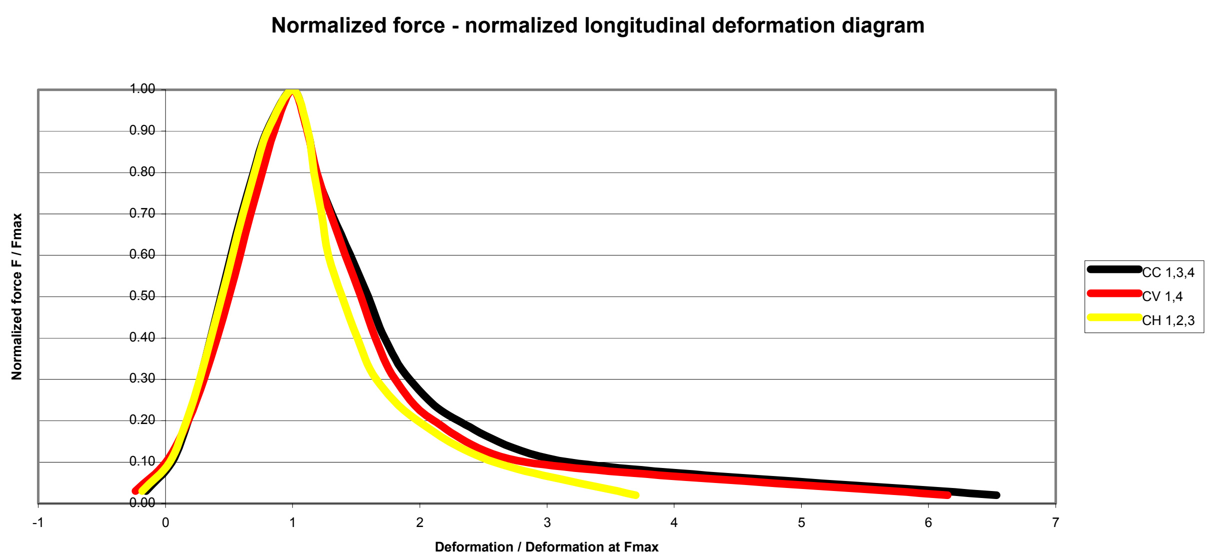

Fig. 5.7: Average lines from the test results for force – longitudinal deformation measurements: normalized force F / F_{max} – normalized deformation diagram

5.2 Discussion of the data

5.2.1 Load – longitudinal deformation diagrams

As can be seen in fig. 5.5, the peak load of the cylinders cast in moulds is about 20 kN higher than that of those drilled from bigger blocks of concrete. The direction of drilling (vertically or horizontally) did not make a difference concerning the peak load.

Normalizing the force to F / F_{max} and the deformation to Deformation / Deformation at F_{max} allows to compare the shape of the curves (see fig. 5.7). In the ascending branch, all three production methods show nearly identical behavior; the curves nearly coincide. In the descending branch, the cylinders cast vertically in a plastic tube (CC) and those drilled vertically from a bigger block (CV) showed nearly identical behavior. The only difference is a slightly steeper descending branch of the curve of the vertically drilled cylinders compared to the vertically cast ones. The deformation at loads lower than ten percent of the maximum load is nearly identical for the two curves.

The horizontally drilled cylinders (CH) exhibited a *slightly* different post-peak behavior. The descending branch is slightly steeper than that of the vertically drilled (CV) and the vertically cast (CC) cylinders. Furthermore, the specimens failed at lower deformations. The horizontally drilled (CH) specimens thus had the lowest ductility. This difference is due to the fact that because of concreting and compacting, the fibers are preferably oriented in the direction of the compressive loading and therefore are not as effective in reducing crack initiation and crack propagation due to transversal stresses as they would if they were oriented perpendicular to the loading direction.

The differences in the curves are very small. It can therefore be stated that (neglecting these slight differences) any of the above described production methods is suitable for manufacturing test specimens for uniaxial compression tests. If one decides on a particular production method, he needs to be aware of the fact that the results will be slightly different for other production methods.

If one bases design proposals on the horizontally drilled (CH) cylinders, he will be on the safe side and still have reserves in peak load as well as post-peak ductility.

Comparing figs. 5.2 to 5.4, it can be stated that the specimens that were not sawn from a block of concrete but cast vertically had the lowest scatter in the load – longitudinal deformation diagram. They showed nearly the same behavior in the ascending branch of the load – deformation curve and in the strain at maximum load. This is a good argument for using cast specimens in the experiments.

Concrete spalling was not expected to be as much as it was.
It was expected that the fibers hold the concrete together as they do at higher fiber contents.

As explained in chapter 5.1, the curves were shifted in order to compensate for the effect that at the beginning of loading the grease is pushed out and the test specimen has to find its way. This explains the unstable shape of the curves at the beginning of the tests.

Compressive strength

It was intended to get a B45. Due to higher age (118 instead of 28 days), the compressive strength of the test cubes was 63.2 N/mm^2 in the average. The cylinders (l/d = 4) had a much lower strength of about 31 N/mm^2.

This can in part be explained by the fact that slender test specimens have a lower compressive strength (factor 0.89 to 0.94 for l/d = 4 for concrete without fibers according to Weigler & Karl, 1989, p. 262). Furthermore, the different way of testing the specimens can be expected to be the cause for the difference in strength. One of these differences was that the cube tests were force controlled and the cylinder tests were deformation controlled. A third factor is the larger air entrapment in larger test specimens because air entrapped in the lower part of the specimen has to pass a longer way through the concrete at compaction than air entrapped in the lower part of a small specimen.

The addition of 40 kg steel fibers per m^3 concrete does not influence the compressive strength significantly. This is known from literature; e.g. Maidl [1995, p. 59] and Sato [1999, p. 11].

5.2.2 Eccentricity of the loading

As stated in chapter 4, the eccentricity was below ± 1 mm in most experiments. The graphs given in appendix A6 show the calculated eccentricity as a function of F/F_{max}. At the beginning of the ascending branch, the test specimens had to find their way and the test had to become stable.
At peak load, the eccentricity was within ± 1 mm from the center of the specimen.
From this, we concluded that the test set-up was suitable for uniaxial compression tests.

Causes for the eccentricity
The eccentricity observed is probably caused by the inhomogeneity within the material itself. There were rather large air entrapments (up to a diameter of about 15 mm) in the cylinder. This represents an inhomogeneity within the specimen. After cracking, the specimen itself is even more inhomogeneous than before cracking. With an inhomogeneous material as concrete this will always be the case and it will always be a relevant factor in experiments with rather small test specimens. When the ratio of specimen size to air entrapment size increases, the influence of such air entrapments decreases.
Other factors that could have caused eccentricities were prevented in this case.
One of them is that the ends of the specimens are sometimes not perfectly parallel and flat. In the experiments described here, the ends were sawn and a so-called capping was put on the ends in a parallel test set-up. Another possibility to even the ends would have been to grind and then polish top and bottom of the specimen.
Another factor that could possibly cause eccentricities is that the hinge assumed at the loading device is not really a hinge and therefore does not load the specimen in the center of the specimen. As shown in fig. 2.1, the point at which the load goes into the specimen could move to a point different from the center of the circle.

5.2.3 Lateral deformation

As a test specimen is pushed, it shows deformation in the longitudinal as well as in the lateral direction. It is expected to deform according to the Poisson's ratio in the lateral direction.

5.2.3.1 Lateral deformation measured in the middle of the specimens (LVDT 05 to 08)

The pushing of all the LVDTs measuring the lateral deformation is due to the fact that cracks develop.

As can be seen in fig. 4.7, the diameters calculated from the deformations measured by LVDT 05 and 07 and LVDT 06 and 08 respectively, are nearly the same. This was expected because the 4 LVDTs measure the deformation of the test specimen at the same height.

5.2.3.2 Lateral deformation measured on top and bottom of the specimens (LVDT 09 and 10)

Failure usually occurred on one end of the specimen, not in the middle.
In case of the vertically drilled (CV) and vertically concreted (CC) specimens this was (as expected) the side of the casting surface.

In case of cylinder CH 1 presented in fig. 4.7, failure occurred on the top of the specimen on which LVDT 09 measured the deformation. LVDT 10 hardly measured any changes.

Side of failure
Past research already showed that the quality of concrete varies over a distance from the finished surface which is equal to the thickness of the cross-section. The side of the test specimen that was in the mould is stronger than the open side [Kooiman, 1998, p. 9-10]. The concrete quality is better on the bottom of the casting form than near the surface. Therefore, this was also expected in these experiments. We observed that the vertically cast specimen indeed failed on the concreting side (see appendix A9). The vertically bored cylinders failed either on the concreting side or in the middle (see appendix A9). The difference in failure mechanism of vertically cast and vertically bored cylinders can in part be explained by the wall effect: in the cast cylinders, the fibers have a two-dimensional distribution at the wall of the tube whereas the fibers in the vertically bored cylinders are more or less three-dimensionally distributed.

It is still questionable, however, whether the failure on this side is only due to the weakness of the casting side or whether it was influenced by the load that was applied on this side.

For the horizontally bored cylinders there was no difference in failure behavior of the two cylinders that were bored from the upper part of the block of concrete compared to those of the lower part.

6 Conclusions

The following conclusions are drawn from the results of the 12 uniaxial compression tests:

(1) It could be clearly seen that failure localizes. This is in accordance with earlier research and also with research on concrete without fibers or with low fiber contents.

(2) The test set-up was appropriate for a uniaxial compression test. This was concluded from the low eccentricities.

(3) Vertically and horizontally drilled specimens had about 10% lower load-carrying capacity than the vertically cast specimens.

(4) The horizontally drilled specimens had the lowest ductility. It was slightly lower than that of the vertically cast and vertically drilled cylinders.

(5) Due to the small differences in results it can be stated that there is not one good production method for the specimens. Each method is suitable for manufacturing test specimens for uniaxial compression tests and has its advantages and disadvantages. If one decides to favor a particular production method, he needs to be aware of the fact that the results he will obtain would be slightly different for other production methods.

(6) The specimens that were cast in a plastic cylinder had the lowest scatter in the load – longitudinal deformation diagram. They showed nearly the same behavior in the ascending branch of the load – deformation curve and in the strain at maximum load.

(7) An argument for not using vertically cast specimens is that they preferably fail on the casting side near the loading zone and they tend to crush more. Using horizontally cast or (vertically or horizontally) drilled specimens avoids that failure is likely to occur on one preferred side of the specimen (in the specimen axis).

(8) Casting the specimens horizontally in steel moulds has the extra advantage that the ends of the specimens are directly ready for testing; no extra treatment such as polishing or capping is needed.

(9) It was therefore decided to cast the test specimens for further research (prism tests planned for 2001) rather than saw them from a bigger block of concrete. The prisms will be cast horizontally.

7 Summary

Twelve steel fiber reinforced concrete cylinders were tested, four of which cast, four vertically drilled from a bigger block and four horizontally drilled from a bigger block.
The results of the uniaxial compression tests were compared and it was decided to do further research with horizontally cast specimens.
The test set-up and the test procedure are described in detail.

Acknowledgement

This research project is a part of the project “The use of new materials in bored concrete tunnels” of the program “Underground structures” of Delft Cluster.
The financial support of Delft Cluster is gratefully acknowledged.

The experiments could not have been done without the help of René v.d. Baars, Ton Blom, Erik Horeweg and Ron Mulder. They are gratefully acknowledged.

Special words of thanks are addressed to Albert Bosman from the technical staff for bringing in his excellent technical skills and enthusiasm and to Theo Stijn for making AutoCAD drawings.

References

ACI committee 544 (1988). *Measurement of Properties of Fiber Reinforced Concrete*, ACI Materials Journal, Nov-Dec 1988, p. 583-593

Bekeart product information

BRITE/EURAM Task Report P-89-3275, 1992, Failure Mechanics of Fibre-Reinforced Concrete and Pre-Damaged Structures, Universität Karlsruhe, Institut für Massivbau und Baustofftechnologie

CUR Aanbeveling 35 (1994). *Bepaling van de buigtreksterkte, de buigtaaiheid en de equivalente buigtreksterkte van staalvezelbeton*. CUR Gouda.

Glavind, M. (1992). *Evaluation of the Compressive Behavior of Fiber Reinforced High Strength Concrete*. PhD thesis, Department of Structural Engineering, Technical University of Denmark.

Grimm, R. (1997). *Einfluss bruchmechanischer Kenngrössen auf das Biege- und Schubtragverhalten hochfester Betone*. Deutscher Ausschuss für Stahlbeton, Heft 477, Beuth Verlag GmbH Berlin / Wien / Zürich

Kooiman, A. G. (1997). *Staalvezelbeton in de Tweede Heinenoord Tunnel; het laboratoriumonderzoek*, Laboratory experiments (in Dutch), Stevinrapport no. 25.5-97-7, Delft University of Technology, Netherlands, 1997, p. 32.

Kooiman, A. G. (1998a). *Staalvezelbeton in de Tweede Heinenoord Tunnel; voorkeursoriëntatie vezels ten gevolge van productieproces*, Evaluation of production process of SFRC tunnel segments (in Dutch), Stevinrapport no. 25.5-98-3, Delft University of Technology, Netherlands, 1998, p. 21.

Kooiman, A. G. (1998b). *Schaaleffecten in het nascheurgedrag van staalvezelbeton*, Stevinrapport Conceptrapport, TU Delft

Kooiman, A. G. (2000). *Modelling Steel Fibre Reinforced Concrete for Structural Design*, PhD thesis TU Delft.

Lin, Y. (1999). *Tragverhalten von Stahlfaserbeton*, Deutscher Ausschuss für Stahlbeton, Heft 494, Beuth Verlag Berlin (ISBN 3-410-65694-4)

Lohrmann, G. (1998). *Faserbeton unter hoher Dehngeschwindigkeit*, Massivbau Baustofftechnologie, Karslruhe Heft 33

Maidl, B. R. (1995). *Steel Fibre Reinforced Concrete*, Ernst & Sohn.

Van Mier, J. G. M. (1997). *Fracture Processes of Concrete – Assessment of Material Parameters for Fracture Models*. CRC Press, Boca Raton (FL), 448 pp.

NEN 5956, 1988, Beton - Bepaling van de consistentie van betonspecie – Zetmaat, Concrete – Determination of the consistency of fresh concrete – Slump test, Nederlands Normalisatie-instituut (NNI), Delft

NEN 5957, 1988, Beton - Bepaling van de consistentie van betonspecie – Schudmaat, Concrete – Determination of the consistency of fresh concrete – Flow test, Nederlands Normalisatie-instituut (NNI), Delft

NEN 5962, 1988, Beton en mortel - Bepaling van het luchtgehalte van beton- en mortelspecie met niet poreus toeslagmateriaal (drukmethode), Concrete and mortar – Determination of air content of fresh concrete and mortar with non-porous aggregates (pressure method), Nederlands Normalisatie-instituut (NNI), Delft

RILEM TC 148-SSC: *Strain softening of concrete- test methods for compressive softening, Test method for measurement of the strain-softening behaviour of concrete under uniaxial compression*, Materials and Structures, Vol. **33**, July 2000, pp 347-351

Sato. Y. (1999). *Mechanical Characteristics of High Performance Fiber Reinforced Cement Based Composites*, Hokkaido University.

Van Vliet, M.; van Mier, J. G. M. (1995). *Concrete Under Uniaxial Compression*, Stevinrapport 25.5-95-9, Delft University of Technology, 109 pp.

Appendices (Tables and Figures)

A1 Concrete mix

A2 Plan for drilling the cylinders

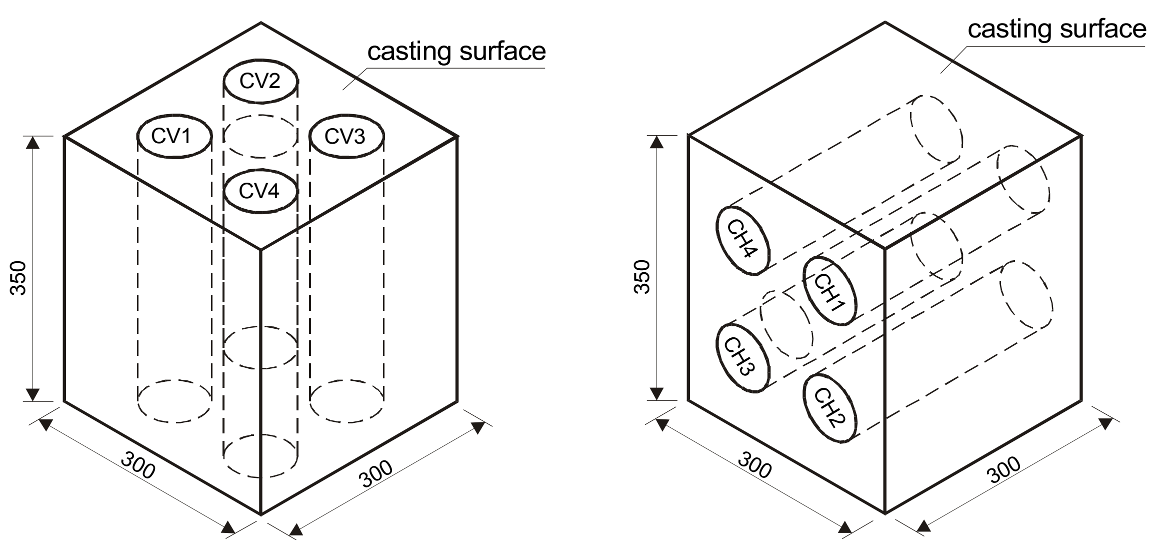

A3 Table Names of the cylinders

Name	Description		
CC 1	cylinder	cast in a plastic tube	number 1
CC 2	cylinder	cast in a plastic tube	number 2
CC 3	cylinder	cast in a plastic tube	number 3
CC 4	cylinder	cast in a plastic tube	number 4
CV 1	cylinder	vertically drilled	number 1
CV 2	cylinder	vertically drilled	number 2
CV 3	cylinder	vertically drilled	number 3
CV 4	cylinder	vertically drilled	number 4
CH 1	cylinder	horizontally drilled	number 1
CH 2	cylinder	horizontally drilled	number 2
CH 3	cylinder	horizontally drilled	number 3
CH 4	cylinder	horizontally drilled	number 4

A4 Proposal for the new testing machine

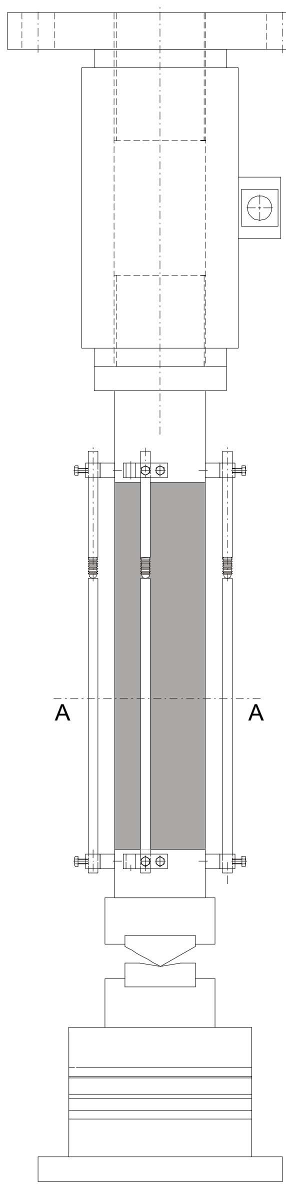

front view

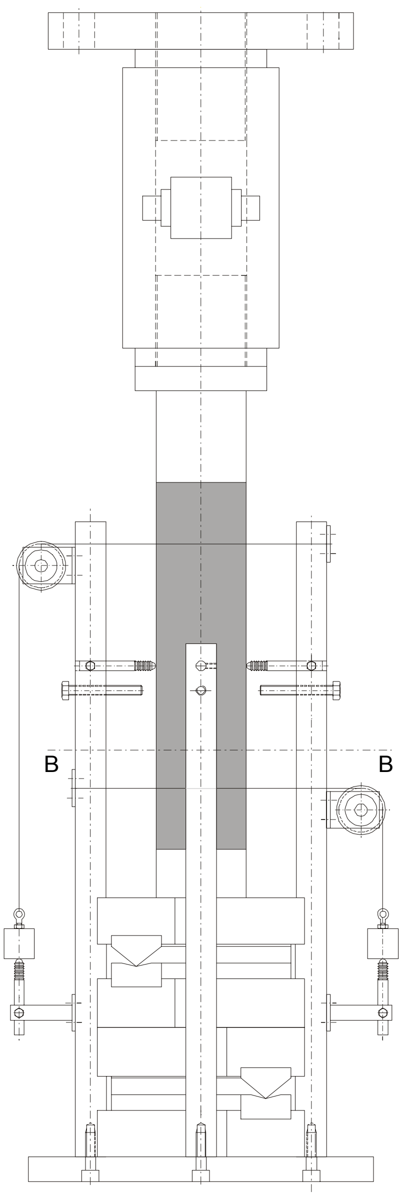

front view 45° rotated

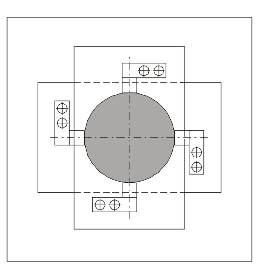

cross section A-A

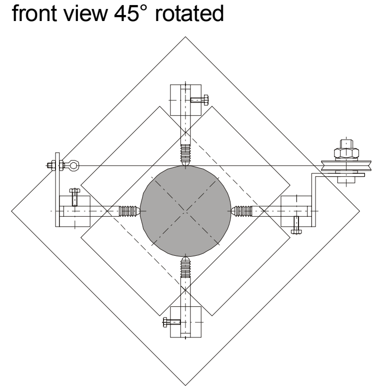

cross section B-B

A5 Load – longitudinal deformation curves of the cylinders (LVDT 01 to 04)

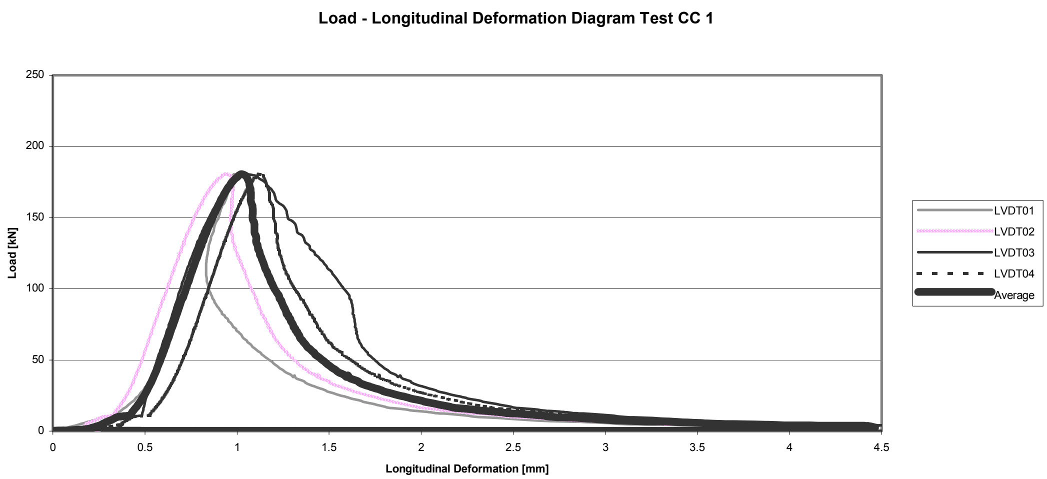

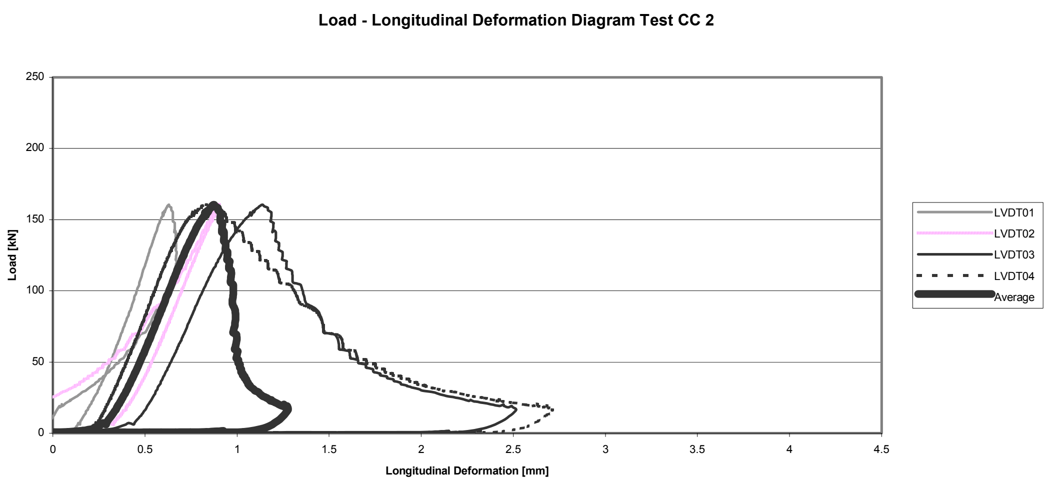

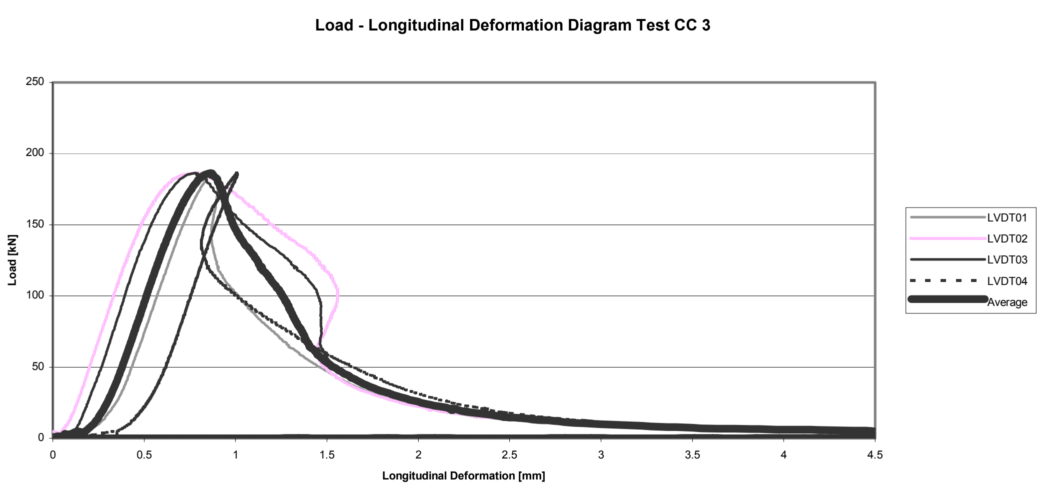

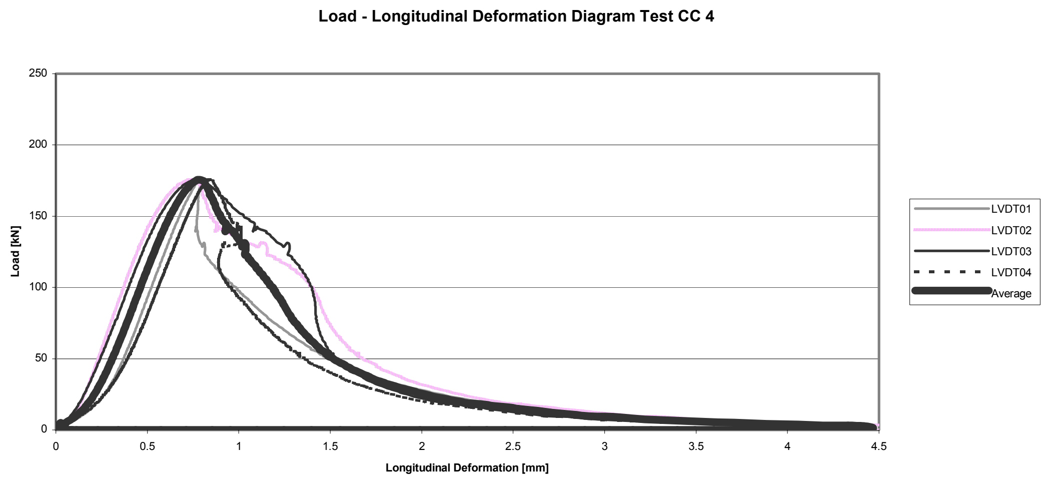
Load - Longitudinal Deformation Diagram Test CC 4
Load [kN]
Longitudinal Deformation [mm]
LVDT01
LVDT02
LVDT03
LVDT04
Average

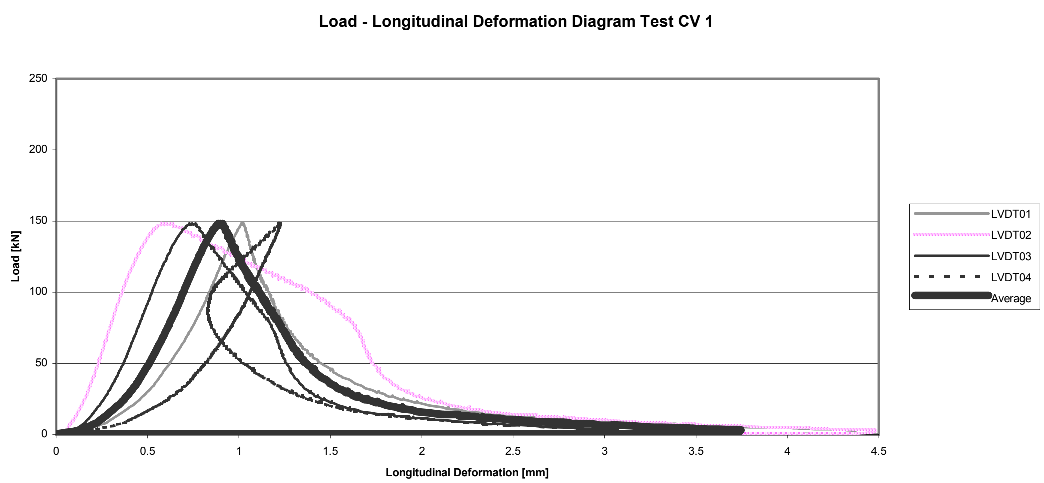
Load - Longitudinal Deformation Diagram Test CV 1
Load [kN]
Longitudinal Deformation [mm]
LVDT01
LVDT02
LVDT03
LVDT04
Average

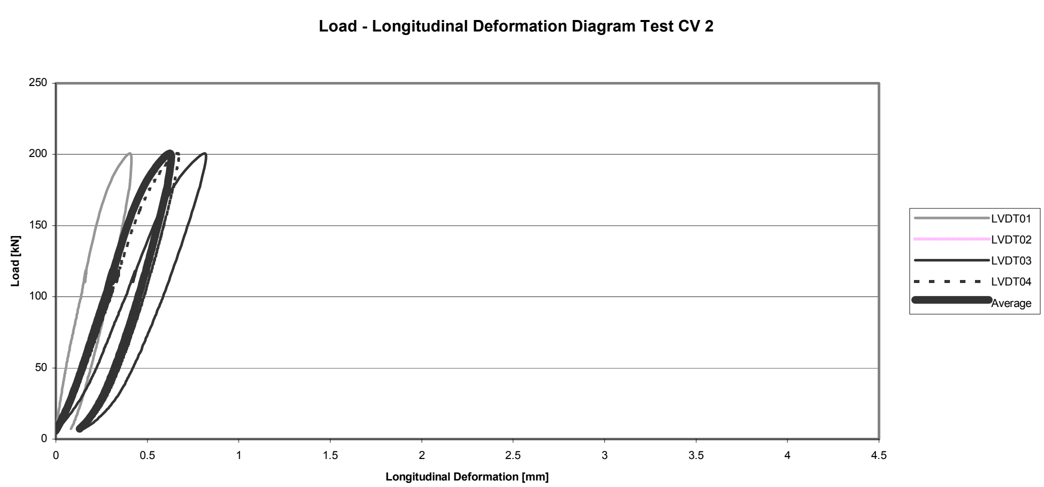
Load - Longitudinal Deformation Diagram Test CV 2
Load [kN]
Longitudinal Deformation [mm]
LVDT01
LVDT02
LVDT03
LVDT04
Average

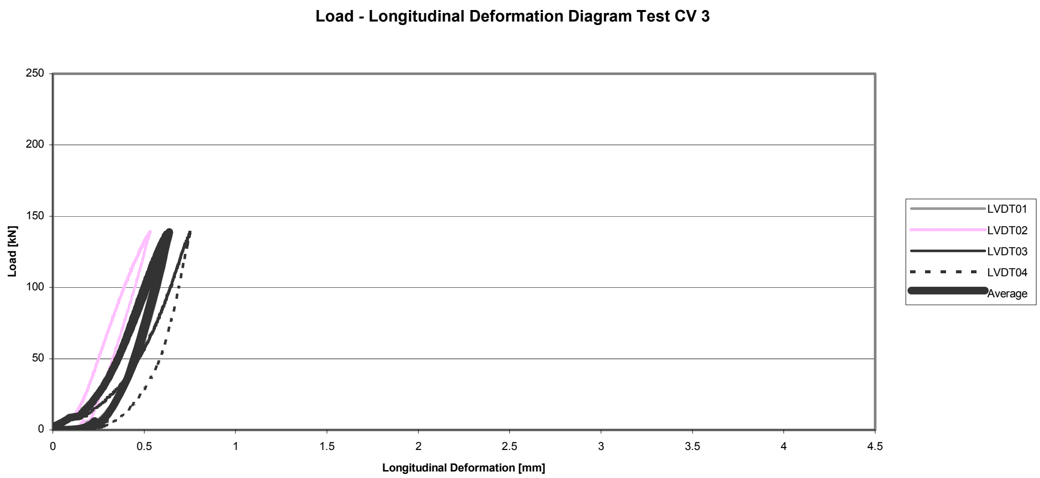
Load - Longitudinal Deformation Diagram Test CV 3
Load [kN]
Longitudinal Deformation [mm]
LVDT01
LVDT02
LVDT03
LVDT04
Average
0
50
100
150
200
250
0
0.5
1
1.5
2
2.5
3
3.5
4
4.5

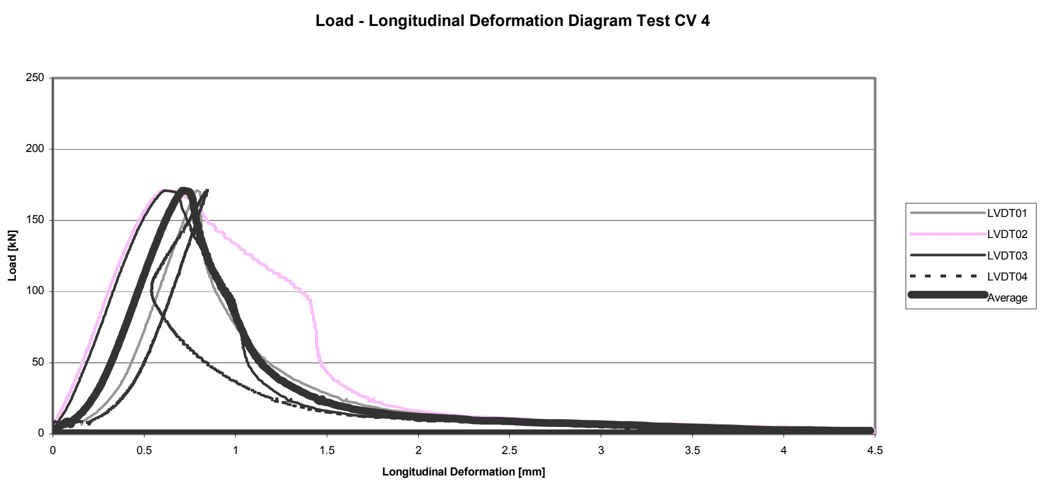
Load - Longitudinal Deformation Diagram Test CV 4
Load [kN]
Longitudinal Deformation [mm]
LVDT01
LVDT02
LVDT03
LVDT04
Average
0
50
100
150
200
250
0
0.5
1
1.5
2
2.5
3
3.5
4
4.5

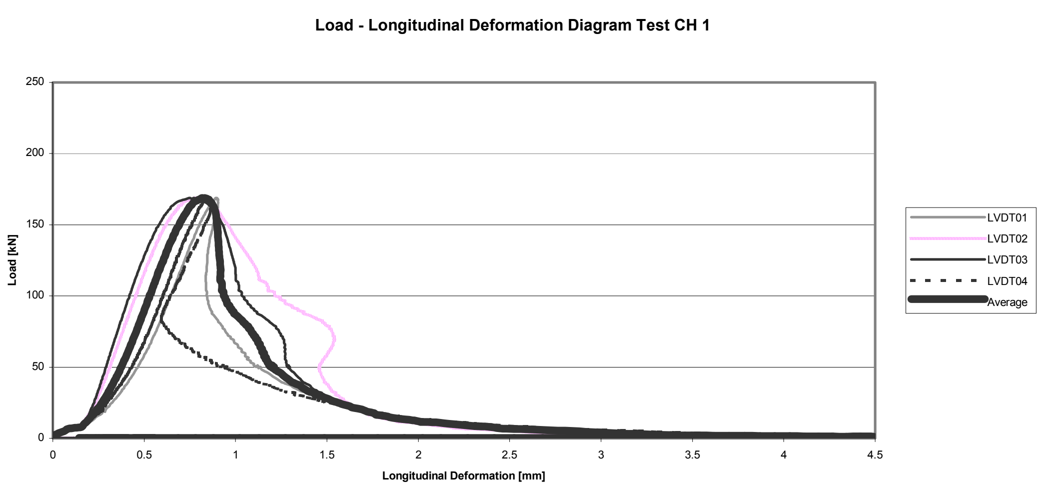
Load - Longitudinal Deformation Diagram Test CH 1
Load [kN]
Longitudinal Deformation [mm]
LVDT01
LVDT02
LVDT03
LVDT04
Average
0
50
100
150
200
250
0
0.5
1
1.5
2
2.5
3
3.5
4
4.5

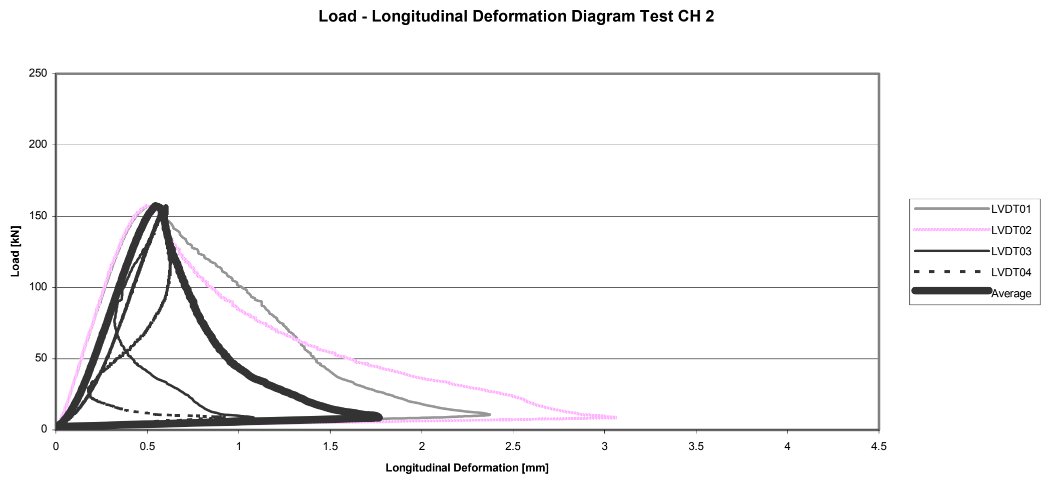
Load - Longitudinal Deformation Diagram Test CH 2
250
200
150
100
50
0
Load [kN]
0
0.5
1
1.5
2
2.5
3
3.5
4
4.5
Longitudinal Deformation [mm]
LVDT01
LVDT02
LVDT03
LVDT04
Average

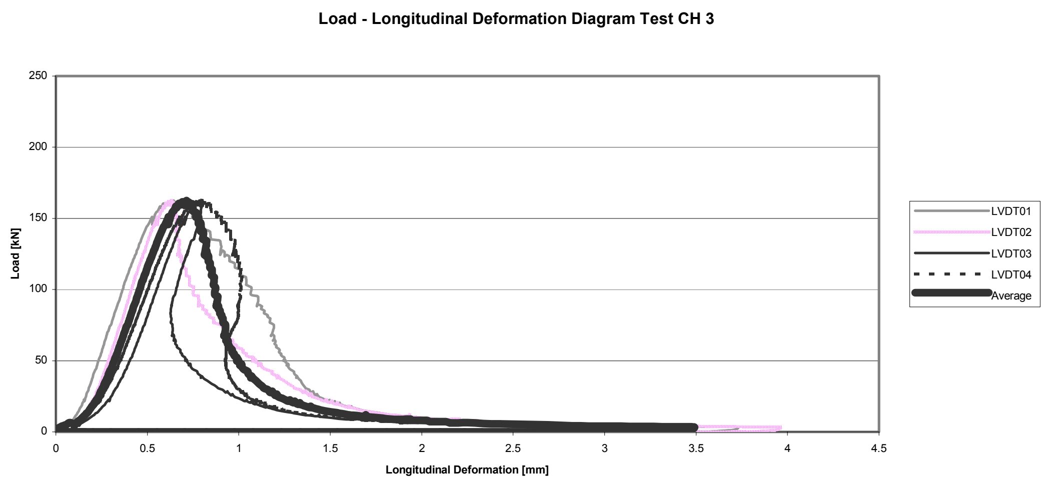
Load - Longitudinal Deformation Diagram Test CH 3
250
200
150
100
50
0
Load [kN]
0
0.5
1
1.5
2
2.5
3
3.5
4
4.5
Longitudinal Deformation [mm]
LVDT01
LVDT02
LVDT03
LVDT04
Average

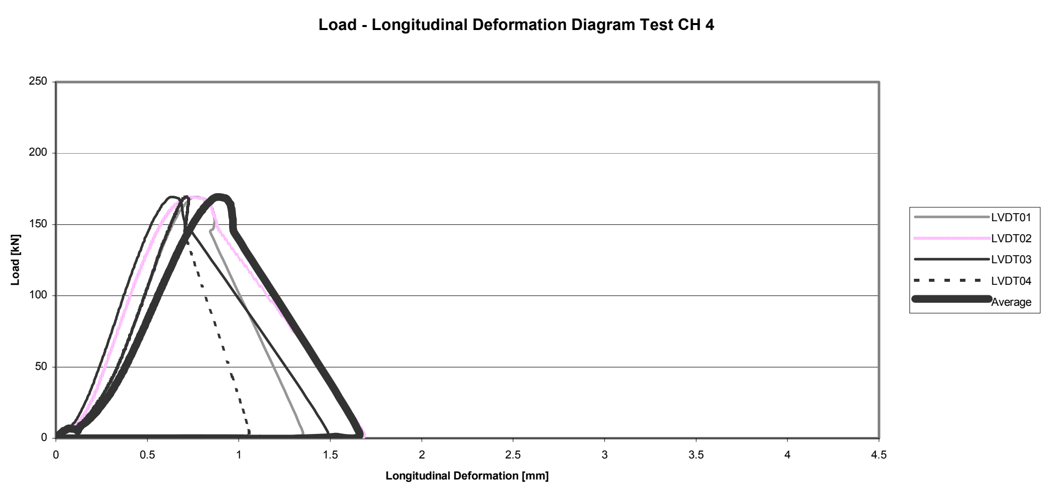
Load - Longitudinal Deformation Diagram Test CH 4
250
200
150
100
50
0
Load [kN]
0
0.5
1
1.5
2
2.5
3
3.5
4
4.5
Longitudinal Deformation [mm]
LVDT01
LVDT02
LVDT03
LVDT04
Average

A6 Load / maximum load– eccentricity diagrams of the cylinder tests

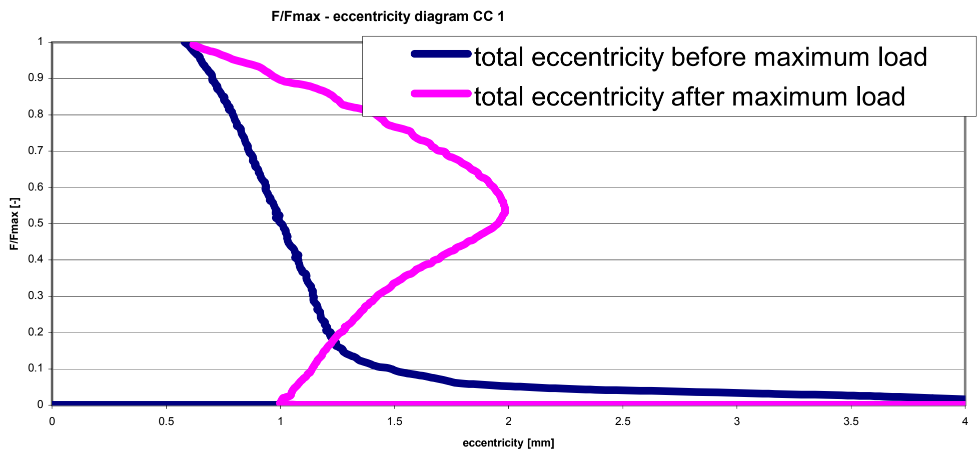

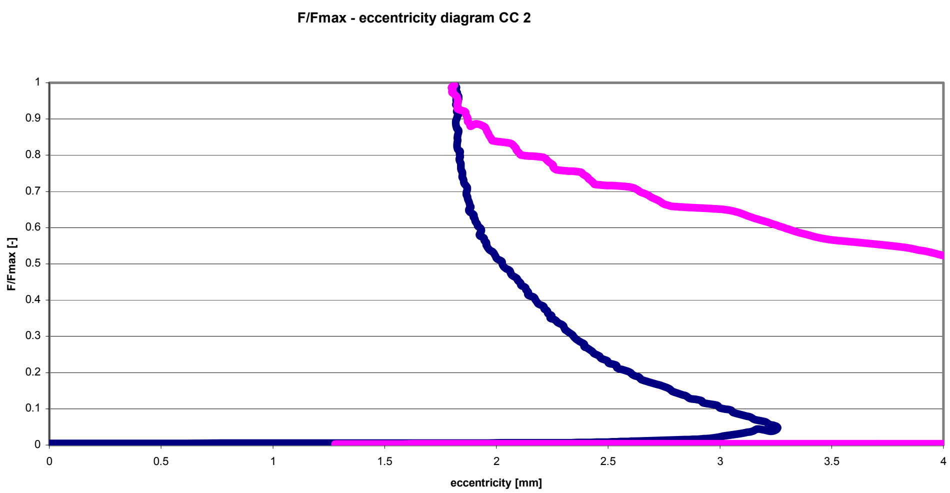

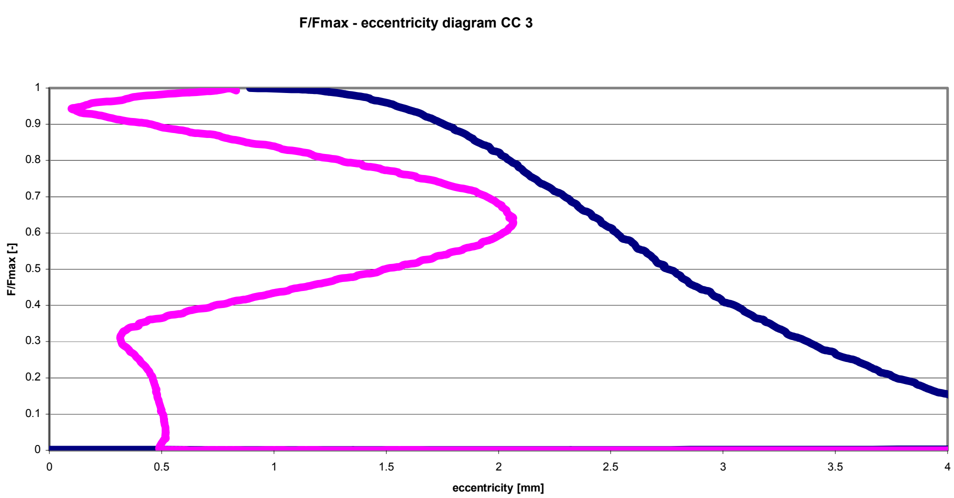

F/Fmax - eccentricity diagram CC 4

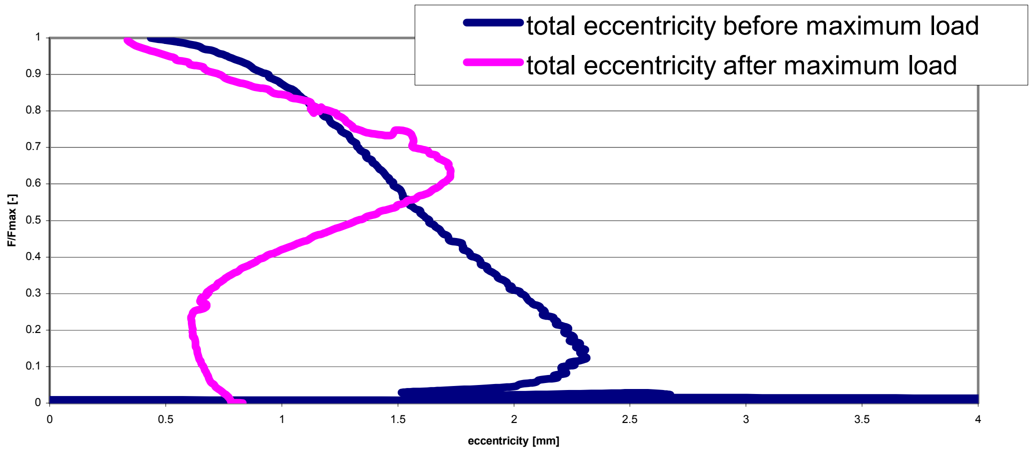

F/Fmax - eccentricity diagram CV 1

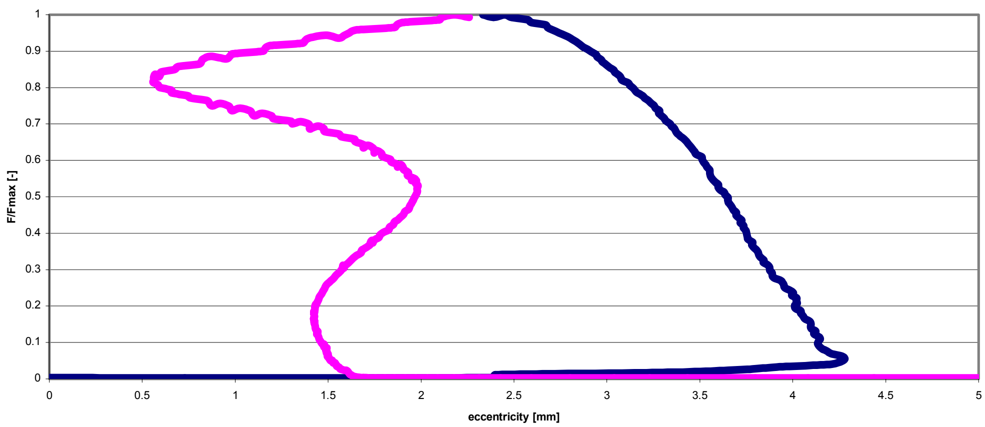

F/Fmax - eccentricity diagram CV 2

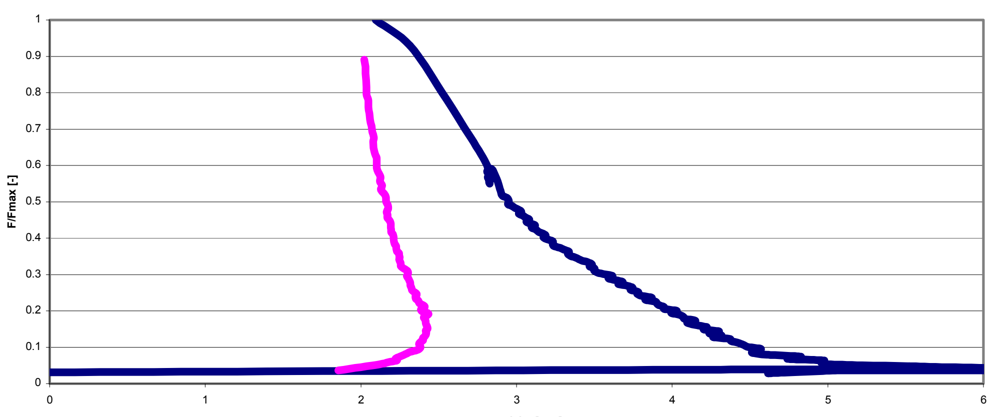

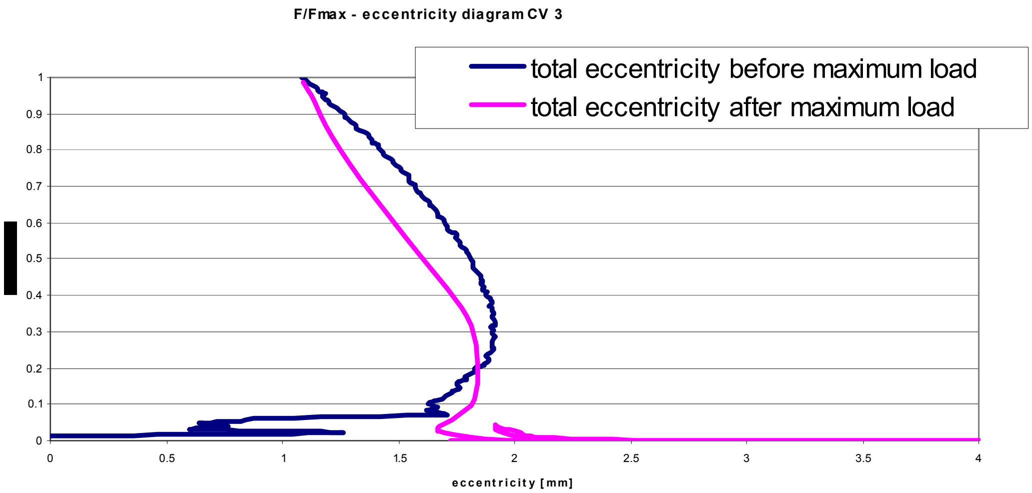
F/Fmax - eccentricity diagram CV 3
total eccentricity before maximum load
total eccentricity after maximum load
[redacted]
eccentricity [mm]

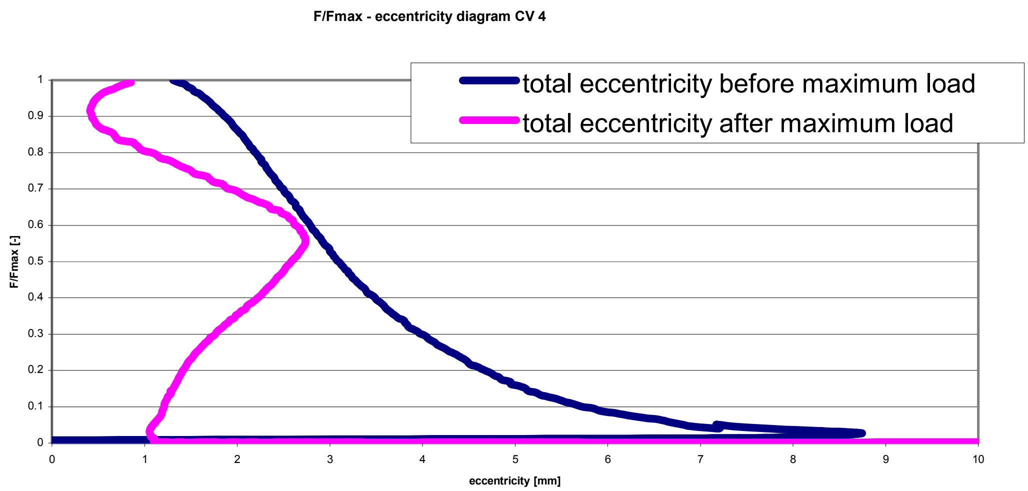
F/Fmax - eccentricity diagram CV 4
total eccentricity before maximum load
total eccentricity after maximum load
F/Fmax [-]
eccentricity [mm]

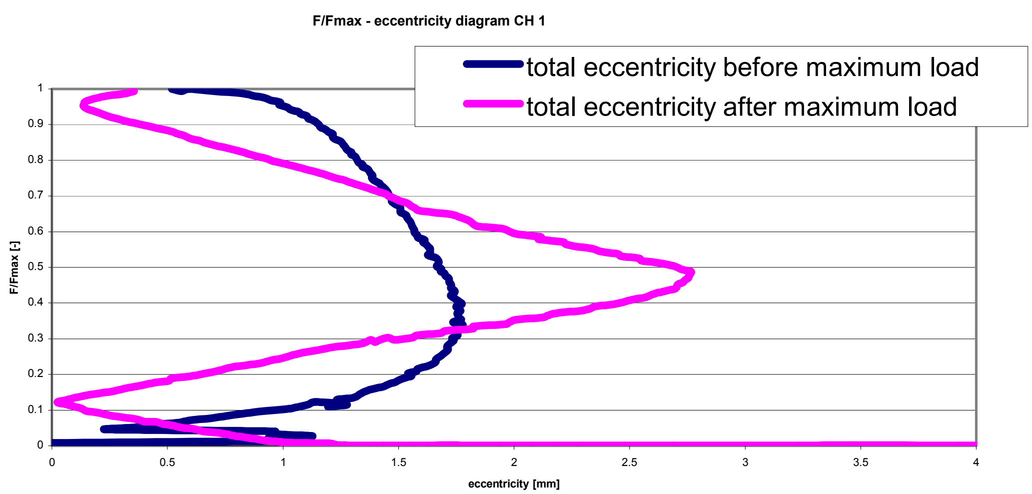
F/Fmax - eccentricity diagram CH 1
total eccentricity before maximum load
total eccentricity after maximum load
F/Fmax [-]
eccentricity [mm]

F/Fmax - eccentricity diagram CH 2

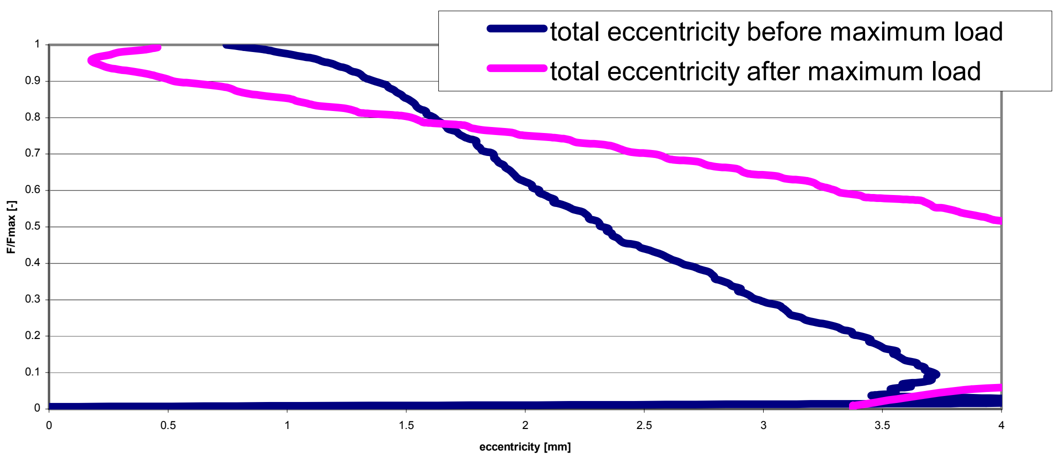

F/Fmax - eccentricity diagram CH 3

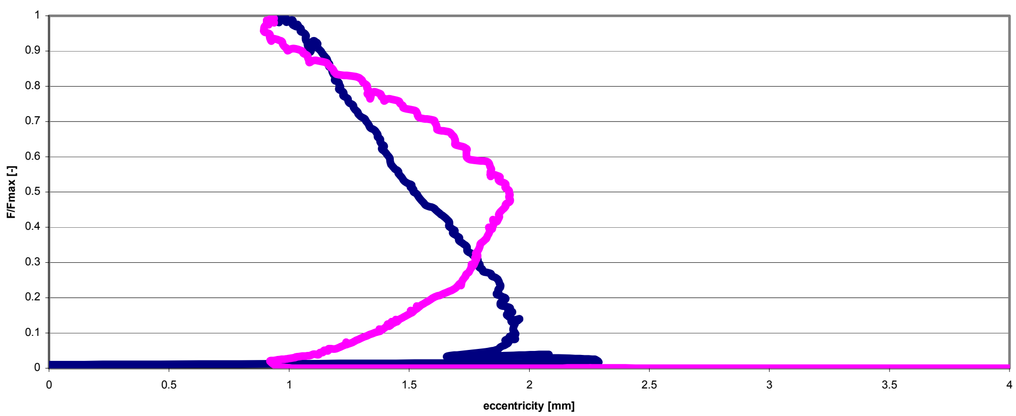

F/Fmax - eccentricity diagram CH 4

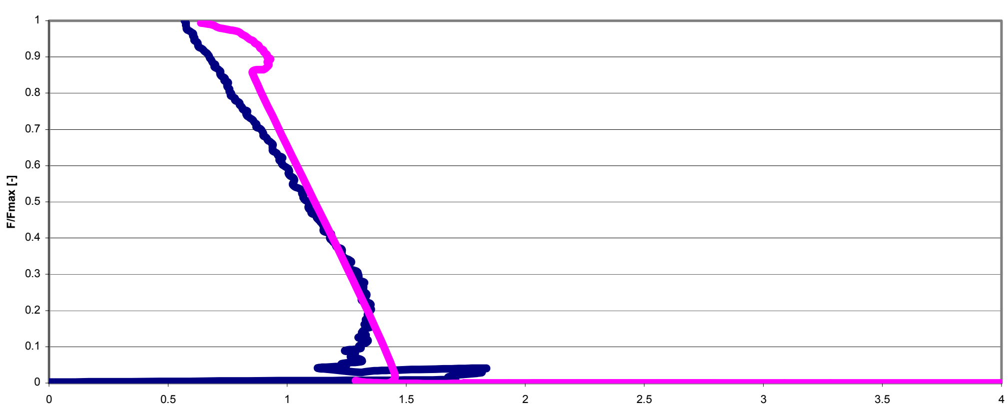

A7 Load – lateral deformation diagrams of the cylinders (LVDT 05 to 08)

Load - lateral deformation diagram CC1

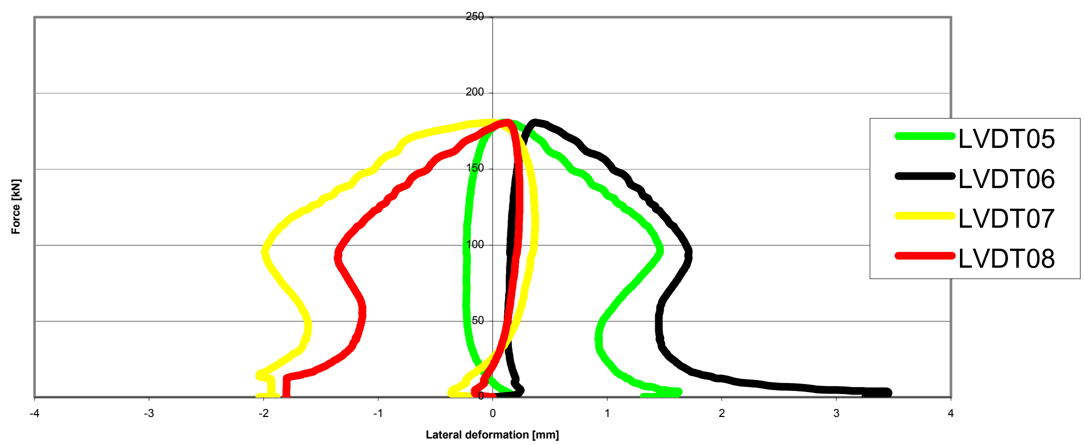

Load - lateral deformation diagram CC2

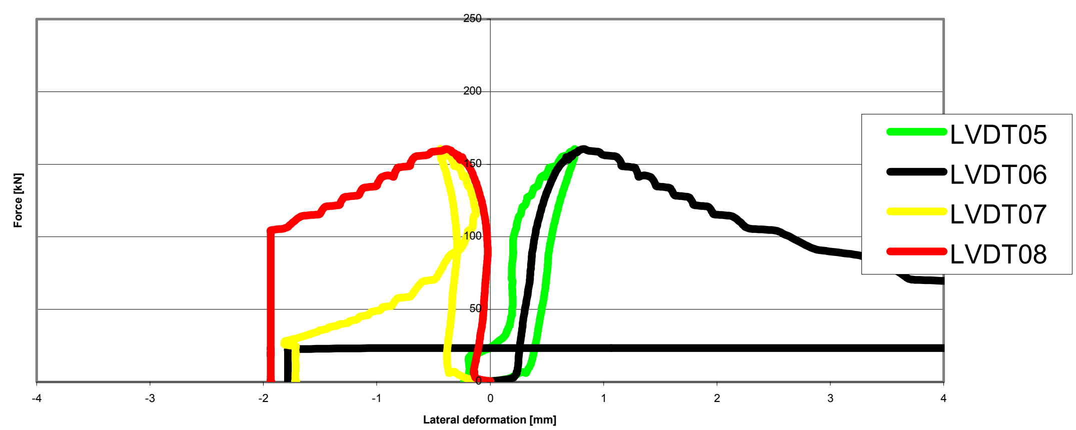

Load - lateral deformation diagram CC3

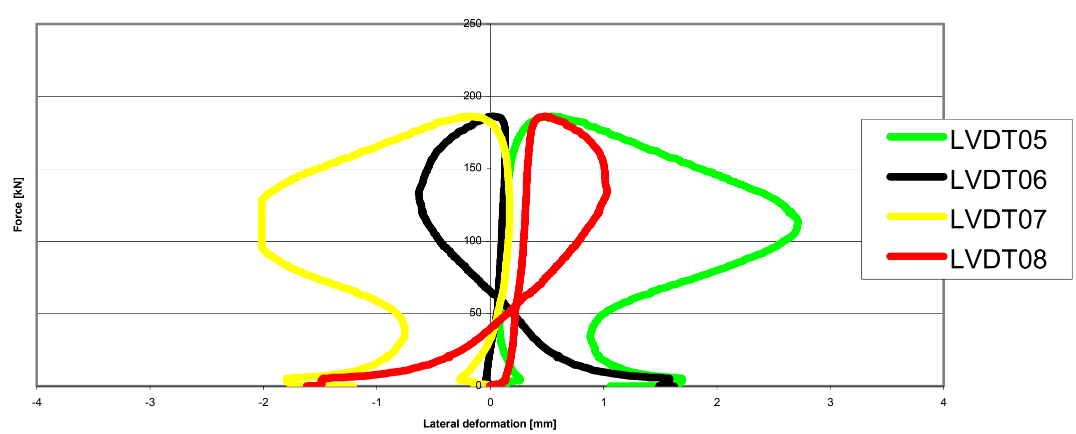

Load - lateral deformation diagram CC4

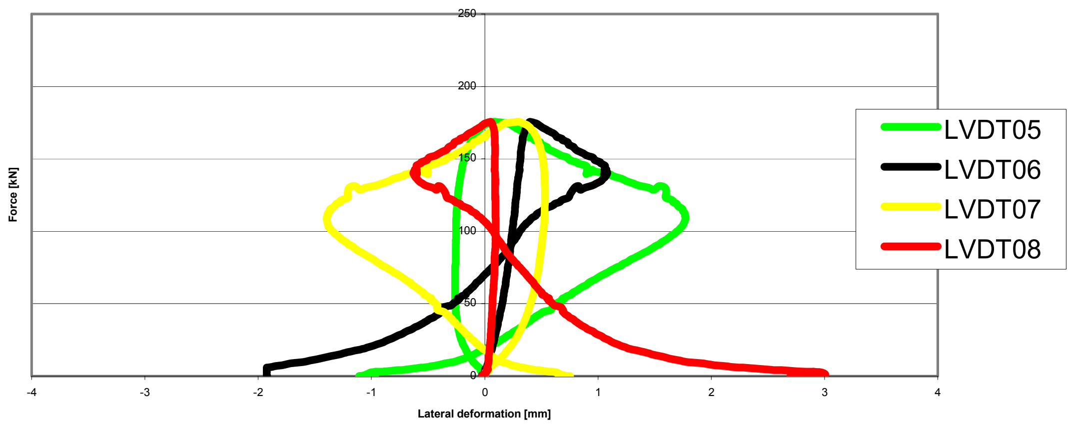

Load - lateral deformation diagram CV1

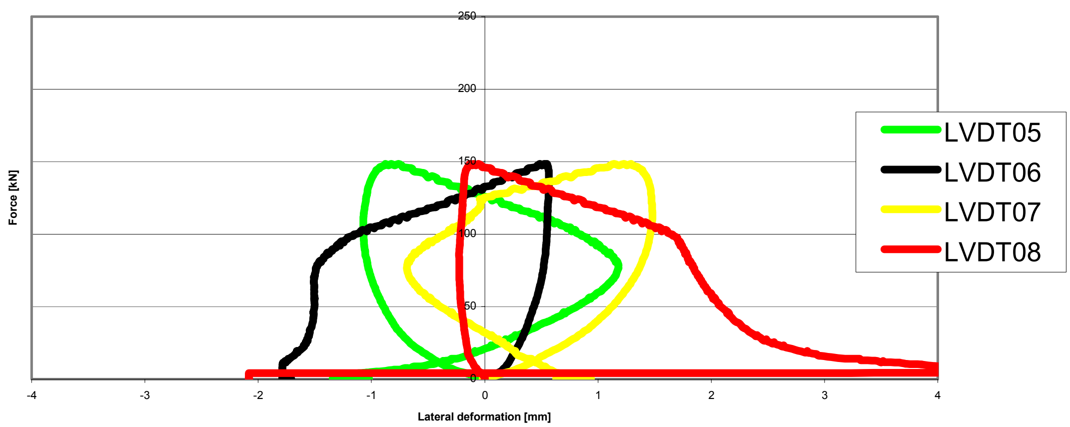

Load - lateral deformation diagram CV2

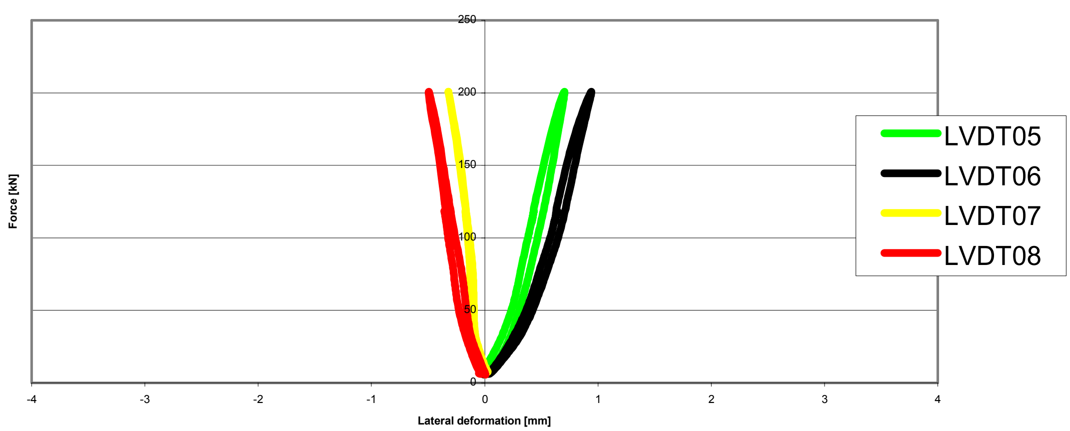

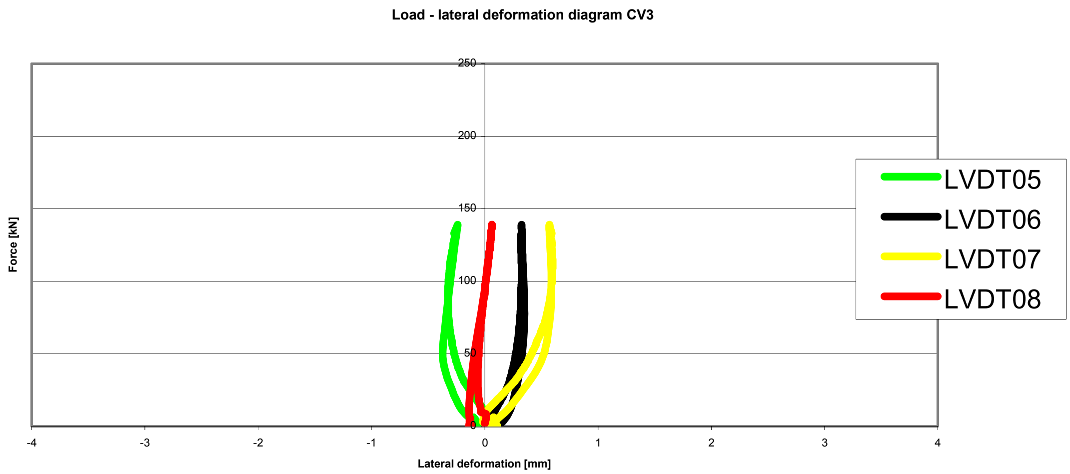
Load - lateral deformation diagram CV3
Force [kN]
Lateral deformation [mm]
LVDT05
LVDT06
LVDT07
LVDT08

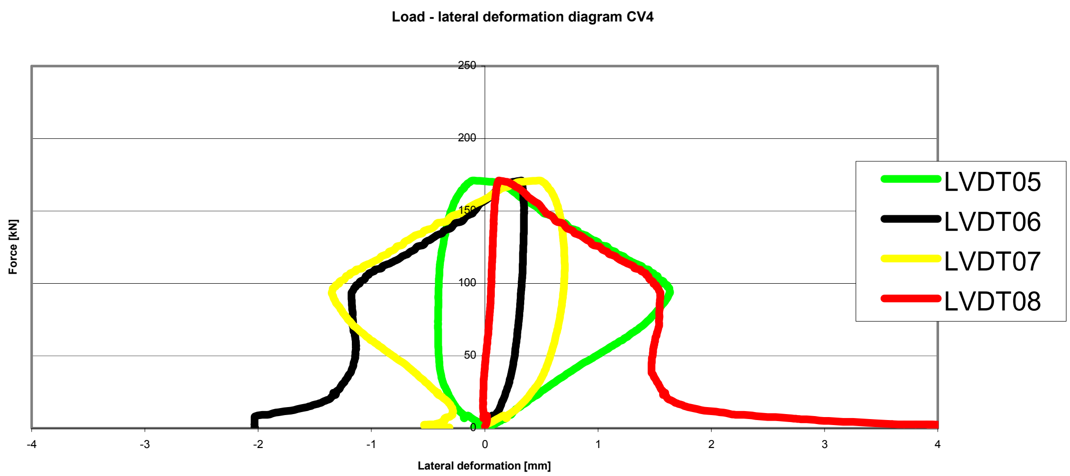
Load - lateral deformation diagram CV4
Force [kN]
Lateral deformation [mm]
LVDT05
LVDT06
LVDT07
LVDT08

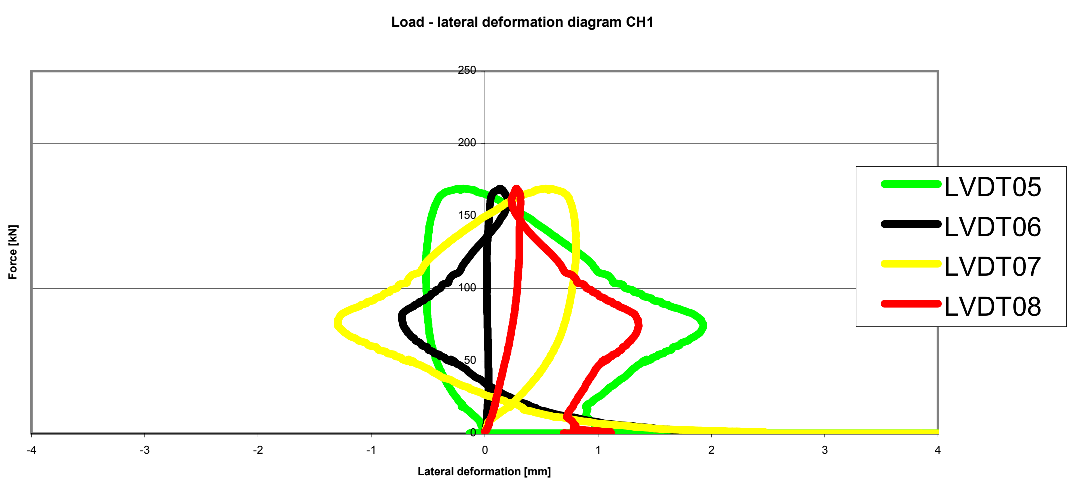
Load - lateral deformation diagram CH1
Force [kN]
Lateral deformation [mm]
LVDT05
LVDT06
LVDT07
LVDT08

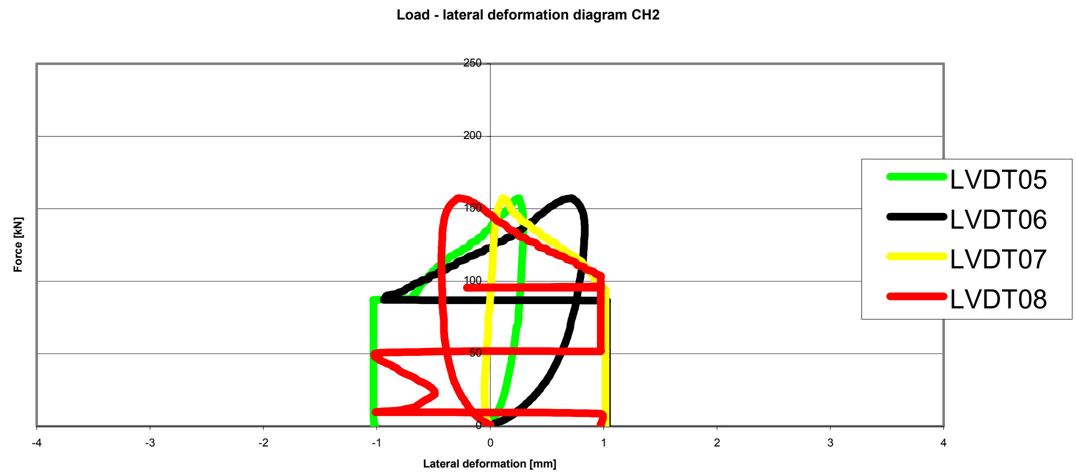
Load - lateral deformation diagram CH2
Force [kN]
Lateral deformation [mm]
LVDT05
LVDT06
LVDT07
LVDT08

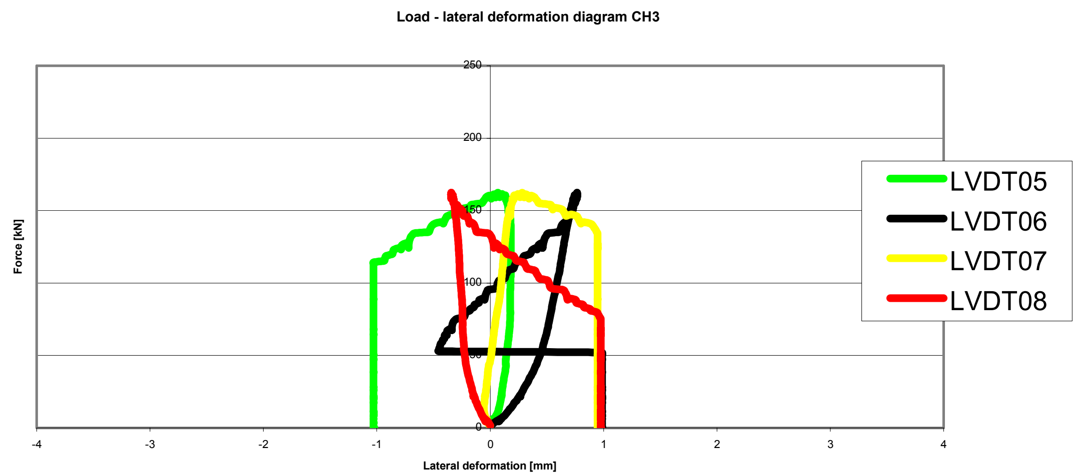
Load - lateral deformation diagram CH3
Force [kN]
Lateral deformation [mm]
LVDT05
LVDT06
LVDT07
LVDT08

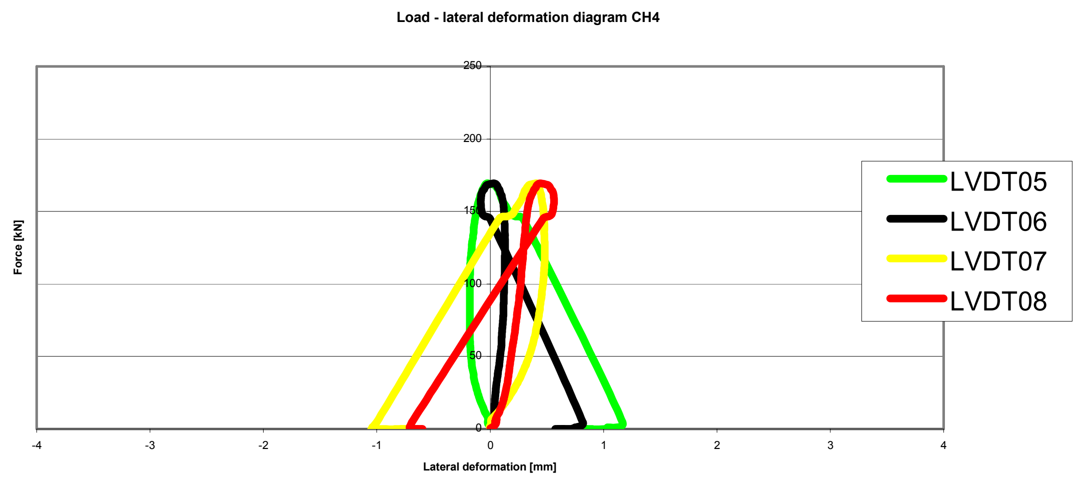
Load - lateral deformation diagram CH4
Force [kN]
Lateral deformation [mm]
LVDT05
LVDT06
LVDT07
LVDT08

A8 Load – diameter diagrams of the cylinders (LVDT 09 to 10)

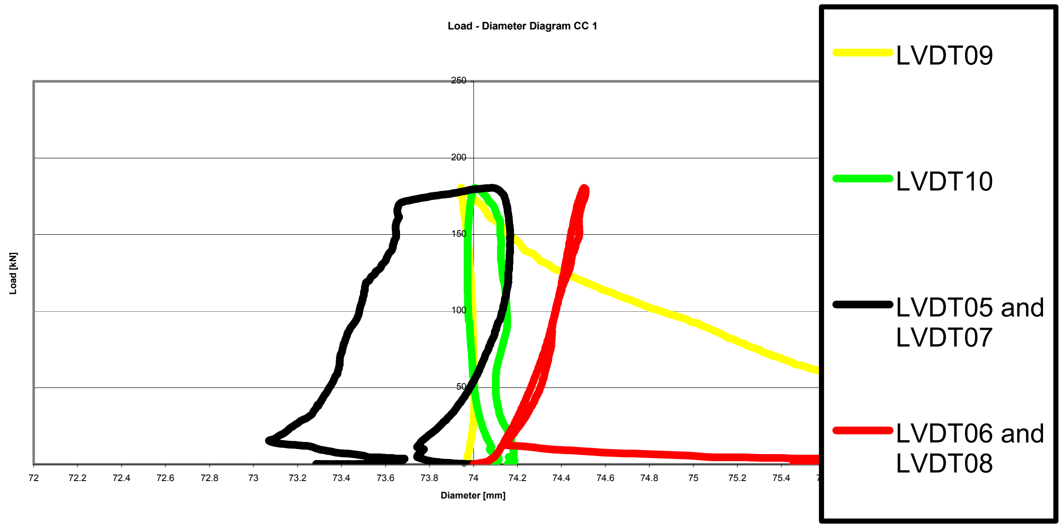

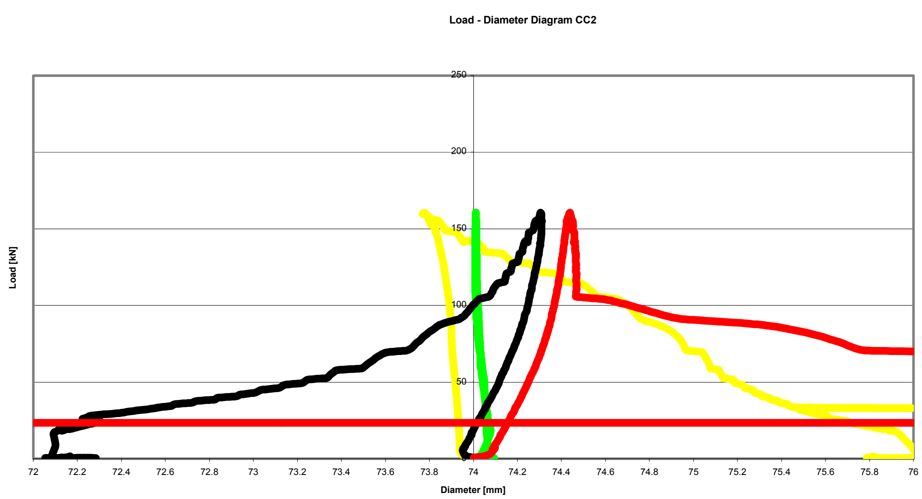

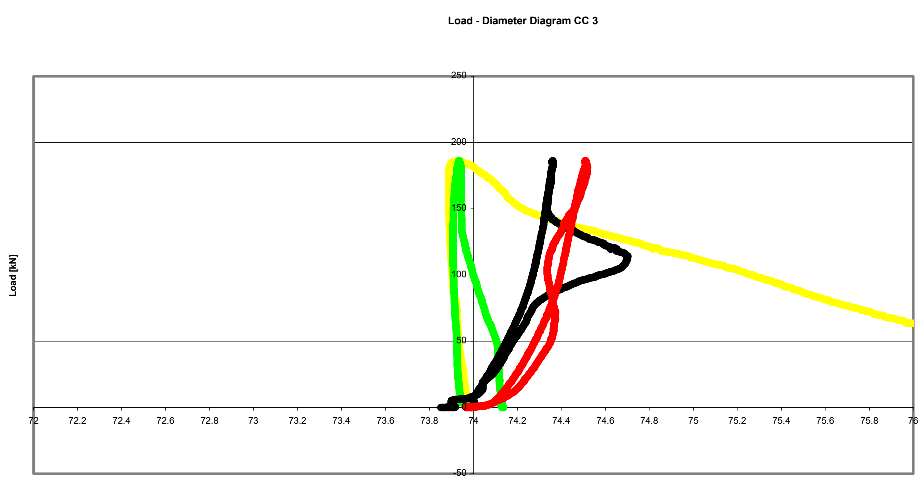

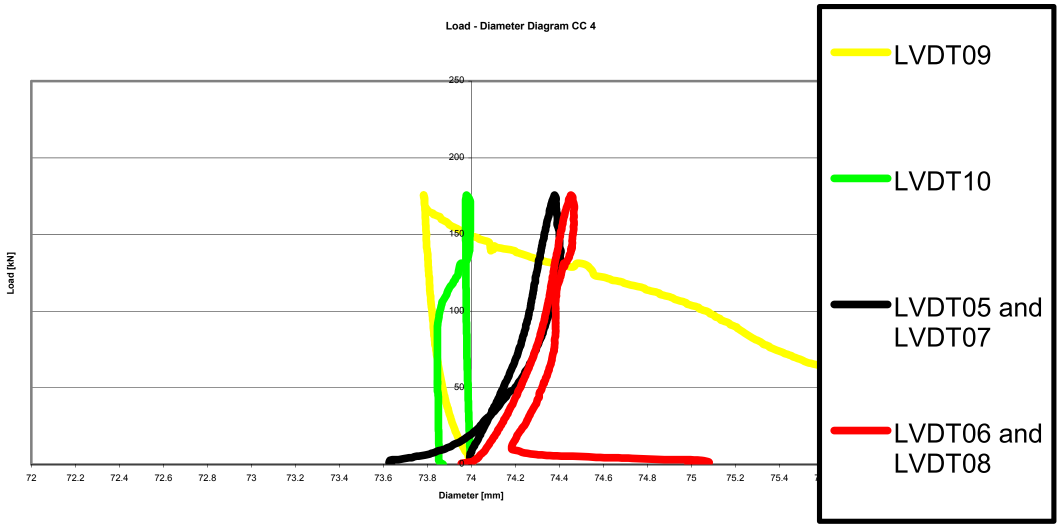
Load - Diameter Diagram CC 4
Load [kN]
Diameter [mm]
LVDT09
LVDT10
LVDT05 and LVDT07
LVDT06 and LVDT08

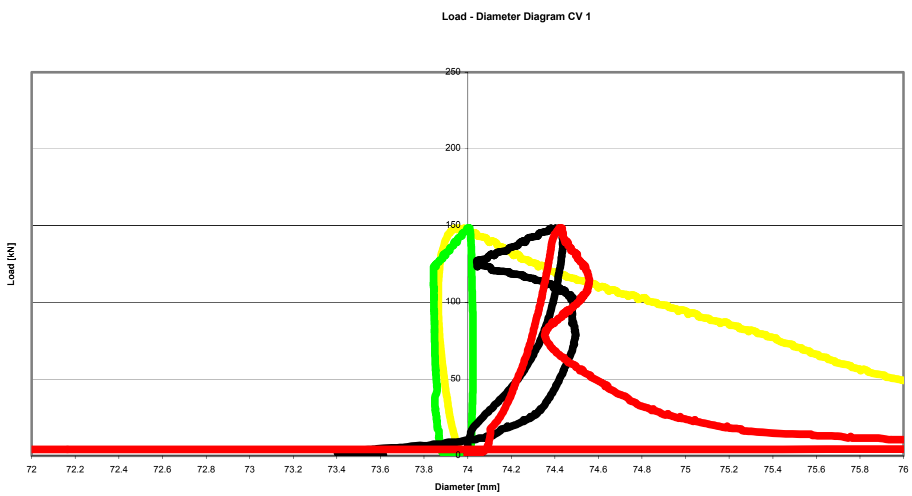
Load - Diameter Diagram CV 1
Load [kN]
Diameter [mm]

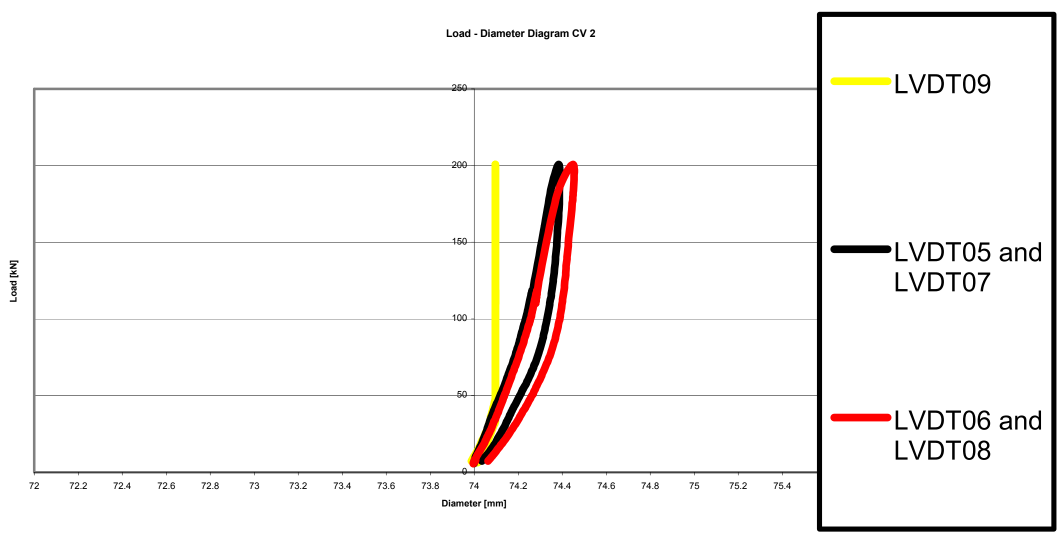
Load - Diameter Diagram CV 2
Load [kN]
Diameter [mm]
LVDT09
LVDT05 and LVDT07
LVDT06 and LVDT08

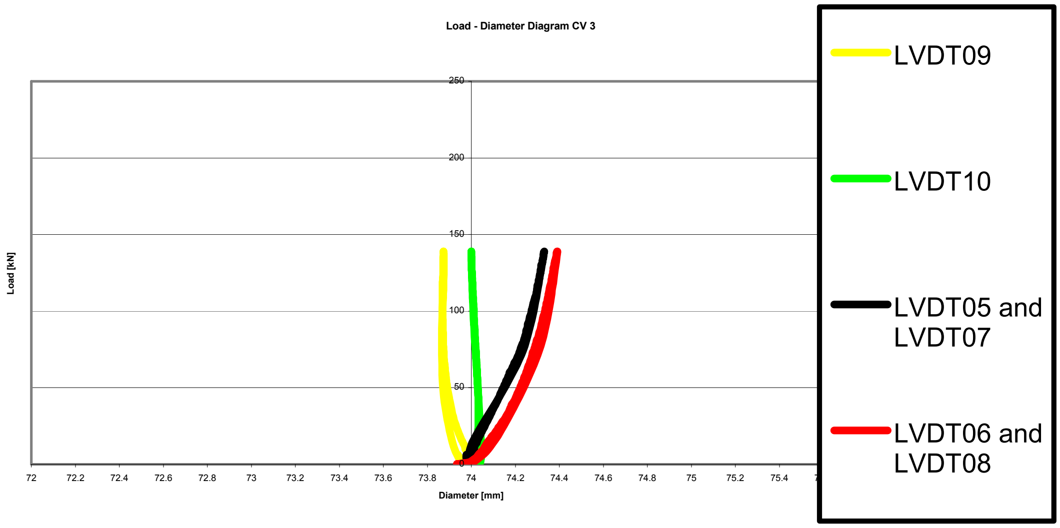
Load - Diameter Diagram CV 3
Load [kN]
Diameter [mm]
LVDT09
LVDT10
LVDT05 and LVDT07
LVDT06 and LVDT08

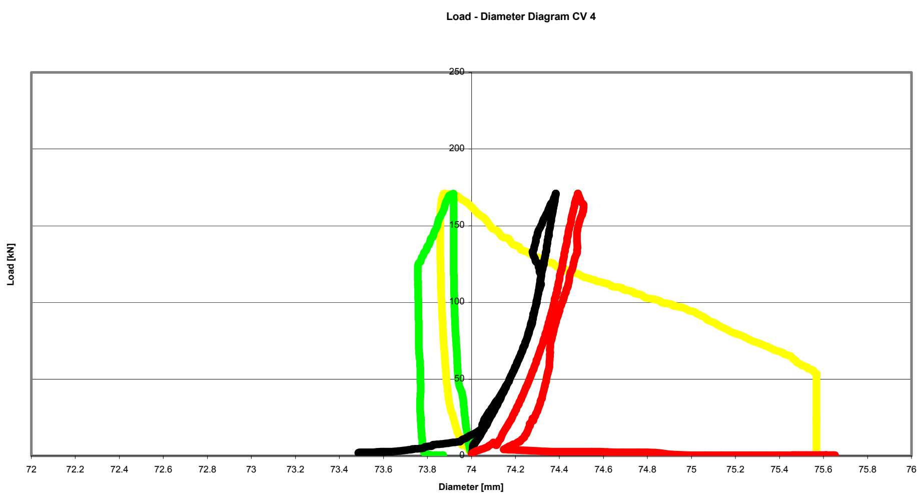
Load - Diameter Diagram CV 4
Load [kN]
Diameter [mm]

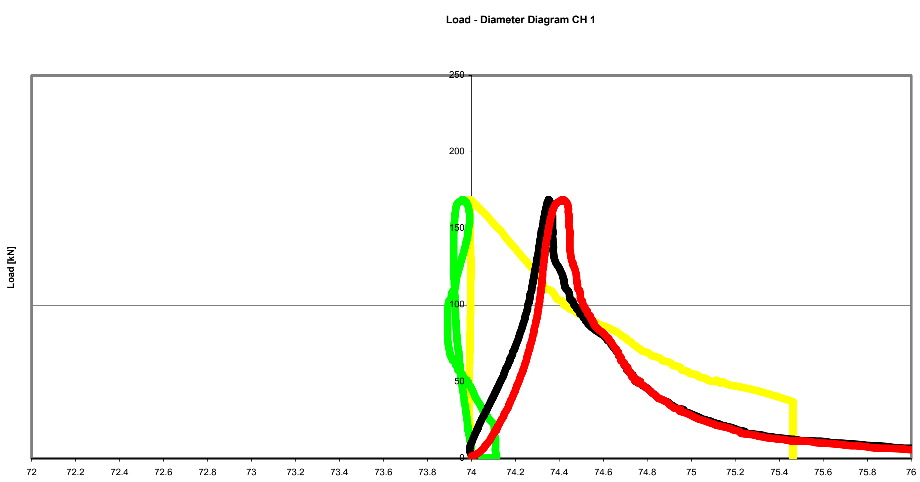
Load - Diameter Diagram CH 1
Load [kN]
Diameter [mm]

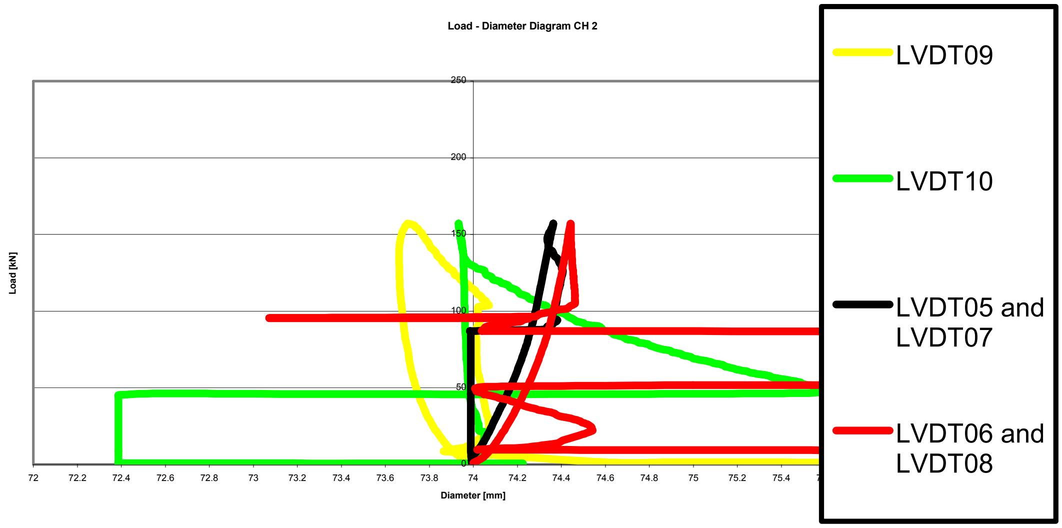
Load - Diameter Diagram CH 2
Load [kN]
Diameter [mm]
LVDT09
LVDT10
LVDT05 and LVDT07
LVDT06 and LVDT08

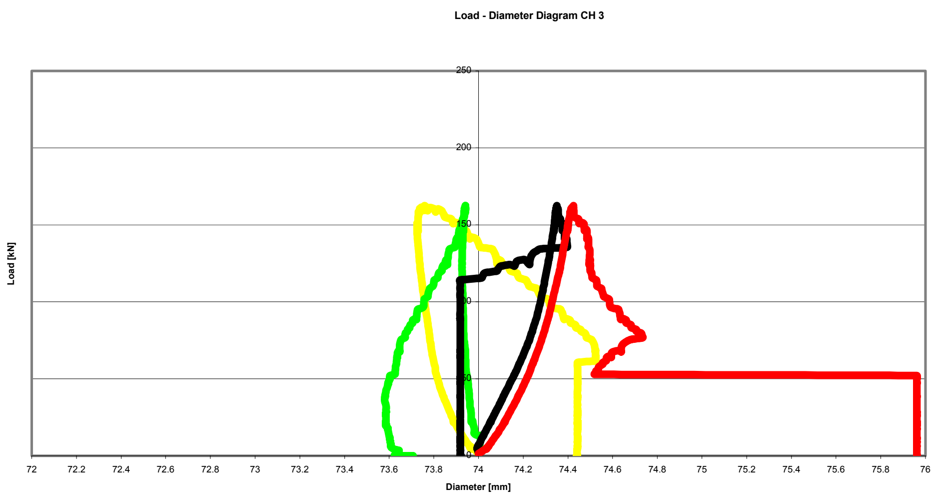
Load - Diameter Diagram CH 3
Load [kN]
Diameter [mm]

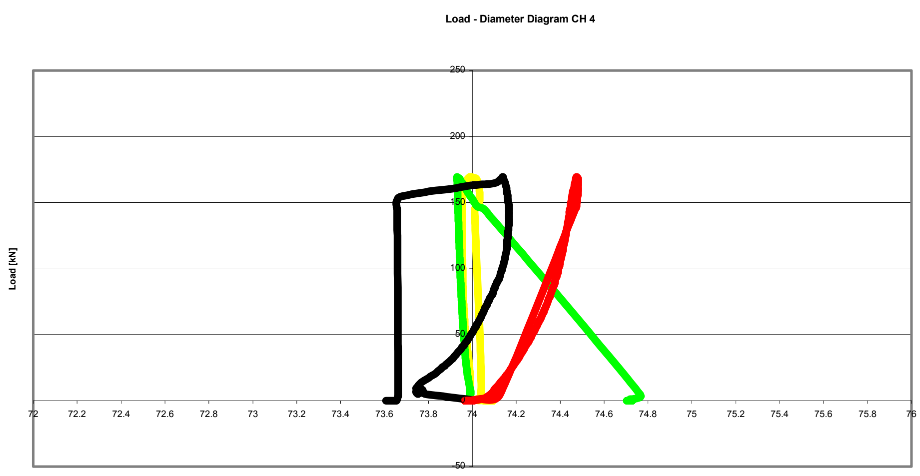
Load - Diameter Diagram CH 4
Load [kN]
Diameter [mm]

A9 Photos of the test specimens after testing

39

40

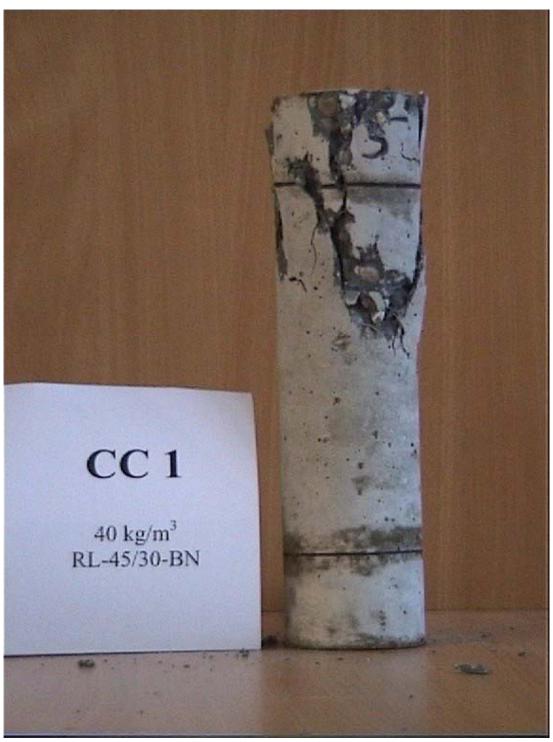

41

42


↑C2
CC 2
40 kg/m3
RL-45/30-BN

43


CC 2
40 kg/m3
RL-45/30-BN

44


CC 2
40 kg/m3
RL-45/30-BN

45


C2
CC 2
40 kg/m3
RL-45/30-BN

46


CC 3
40 kg/m3
RL-45/30-BN

47


CC 3
40 kg/m3
RL-45/30-BN

48


CC 3
40 kg/m3
RL-45/30-BN

49


7
C4
CC 4
40 kg/m3
RL-45/30-BN
51


CC 4
40 kg/m3
52


CC 4
40 kg/m3
RL-45/30-BN
53


7
C4
CC 4
40 kg/m3
RL-45/30-BN
54


CV 1
40 kg/m3
RL-45/30-BN

31


CV 1
40 kg/m3
RL-45/30-BN

32


CV 1
40 kg/m3
RL-45/30-BN

33


CV 1
40 kg/m3
RL-45/30-BN

34

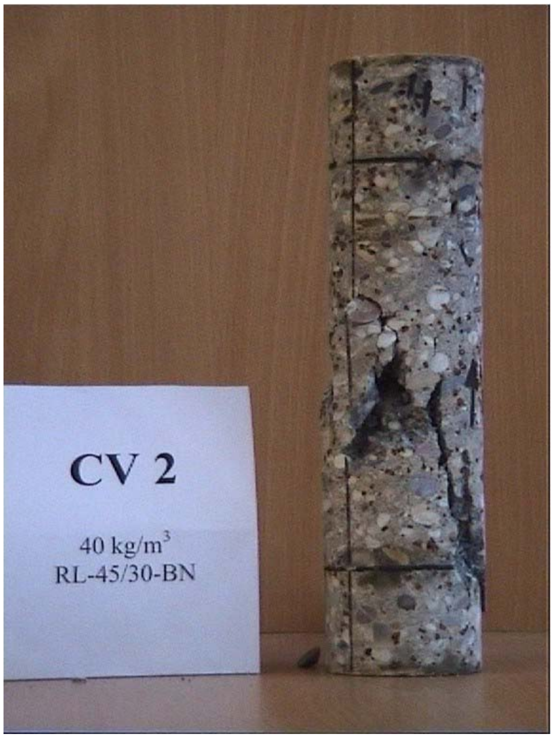
CV 2
40 kg/m3
RL-45/30-BN
21


CV 2
40 kg/m3
RL-45/30-BN
22


CV 2
40 kg/m3
RL-45/30-BN
23


CV 2
40 kg/m3
RL-45/30-BN
24

25

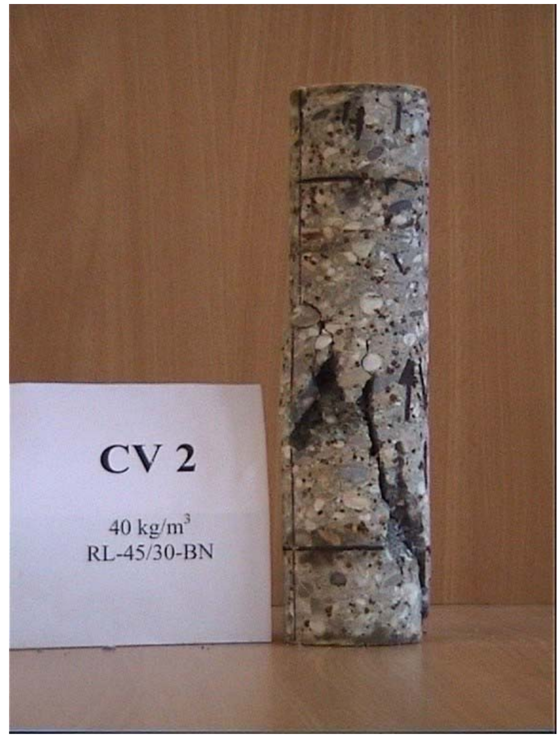

26

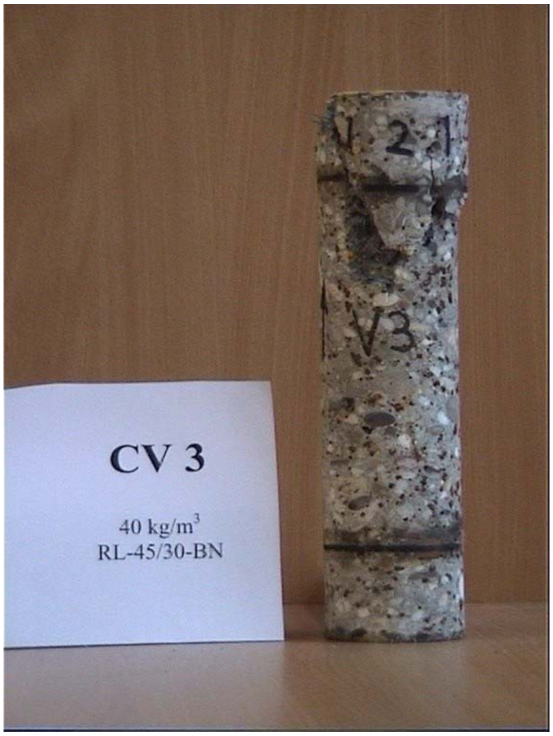
CV 3
40 kg/m^3
RL-45/30-BN

28


CV 3
40 kg/m^3
RL-45/30-BN

29


CV 3
40 kg/m^3
RL-45/30-BN

30

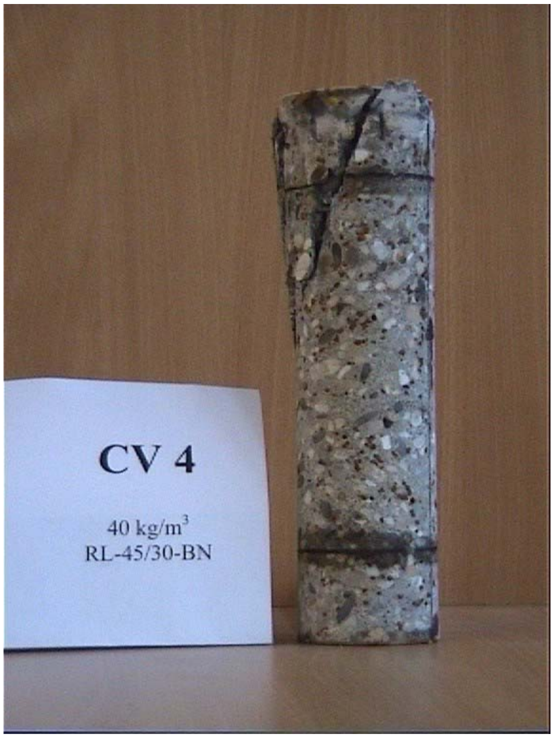
CV 4
40 kg/m3
RL-45/30-BN
35


CV 4
40 kg/m3
RL-45/30-BN
36


CV 4
40 kg/m3
RL-45/30-BN
37

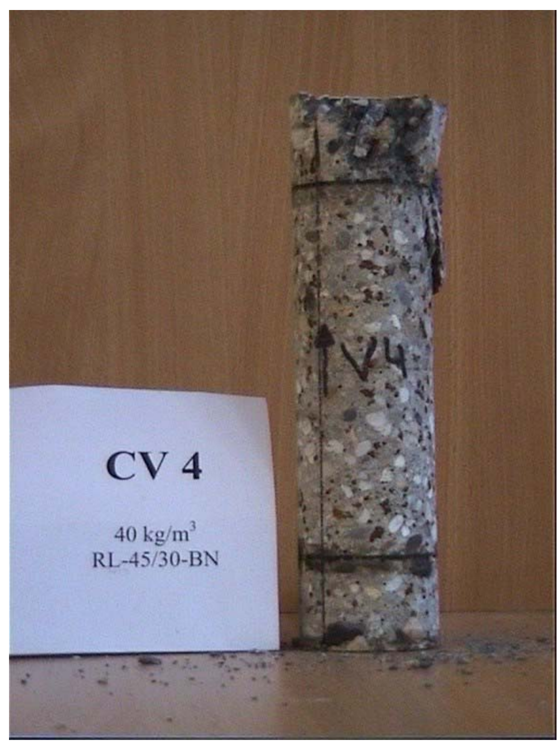
CV 4
40 kg/m3
RL-45/30-BN
38


CH 1
40 kg/m3
RL-45/30-BN
55

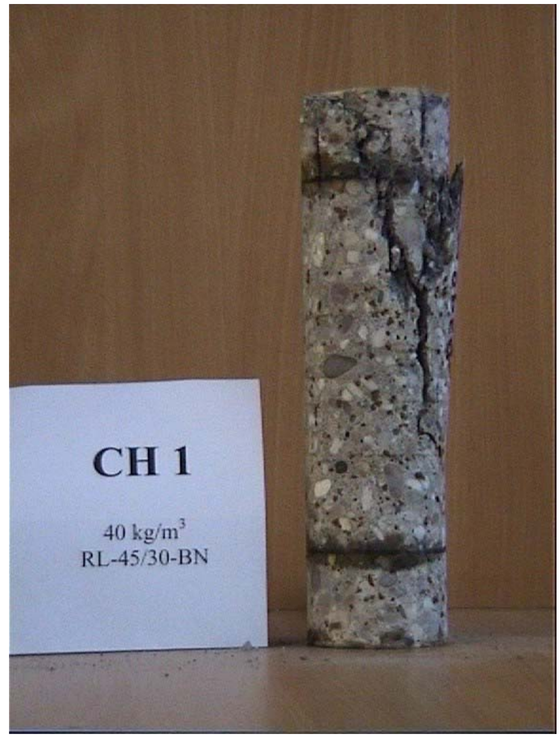
CH 1
40 kg/m3
RL-45/30-BN
56


CH 1
40 kg/m3
RL-45/30-BN
57

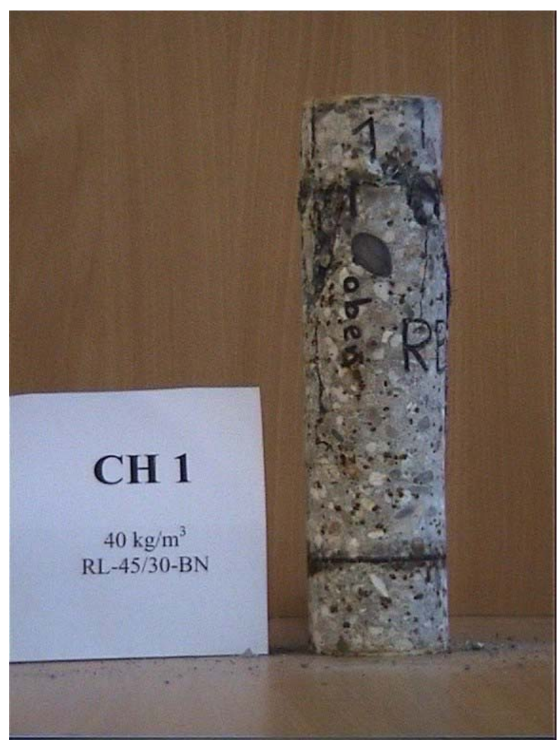
CH 1
40 kg/m3
RL-45/30-BN
58


CH 2
40 kg/m3
RL-45/30-BN
59


CH 2
40 kg/m3
RL-45/30-BN
60


CH 2
40 kg/m3
RL-45/30-BN
61


CH 2
40 kg/m3
RL-45/30-BN
62

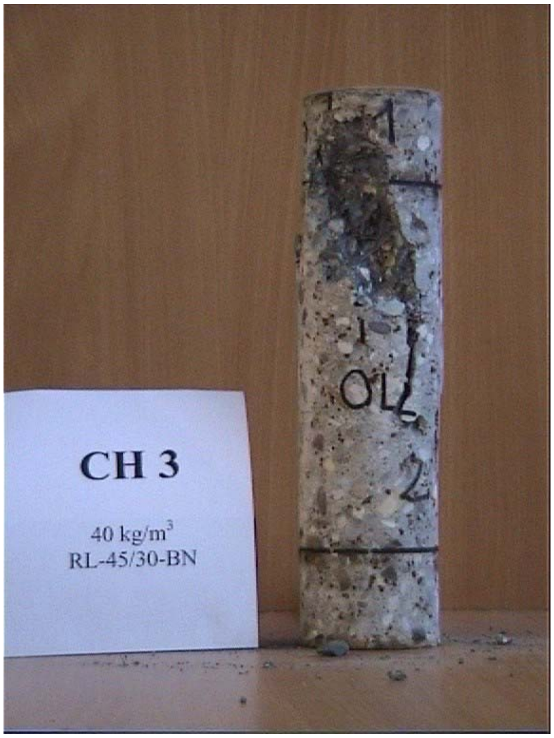
CH 3
40 kg/m³
RL-45/30-BN
63


CH 3
40 kg/m³
RL-45/30-BN
64


CH 3
40 kg/m³
RL-45/30-BN
65


CH 3
40 kg/m³
RL-45/30-BN
66


CH 4
40 kg/m^3
RL-45/30-BN

67


CH 4
40 kg/m^3
RL-45/30-BN

68

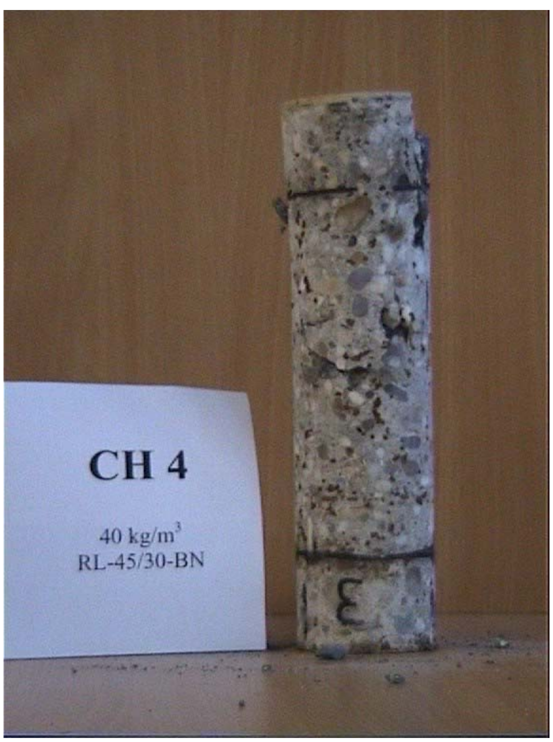
CH 4
40 kg/m^3
RL-45/30-BN

69


CH 4
40 kg/m^3
RL-45/30-BN

70